Methods in isolation and characterization of bovine monocytes and macrophages

Ceciliani F.[a]*, Ávila Morales G.[a], De Matteis G.[b], Grandoni F.[b], Furioso Ferreira R.[c,d], Roccabianca P.[a], Lecchi C.[a]

[a] Department of Veterinary Medicine, Università degli Studi di Milano, Milan, Italy
[b] Research Centre of Animal Production and Aquaculture, Council for Agricultural Research and Economics (CREA), Monterotondo, Rome, Italy
[c] Faculty of Veterinary Medicine, University of Zagreb, Zagreb, Croatia
[d] Institute for Animal Sciences, Physiology and Hygiene Unit, University of Bonn, Bonn, Germany
* Corresponding author at Department of Veterinary Medicine, Università degli Studi di Milano, Milan, Italy
Email address: fabrizio.ceciliani@unimi.it (F.Ceciliani)

Abstract

Monocytes and macrophages belong to the mononuclear phagocyte system and play important roles in both physiological and pathological processes. The cells belonging to the monocyte/macrophage system are structurally and functionally heterogeneous. Several subsets of monocytes have been previously identified in mammalian blood, generating different subpopulations of macrophages in tissues. Although their distribution and phenotype are similar to their human counterpart, bovine monocytes and macrophages feature differences in both functions and purification procedures. The specific roles that monocytes and macrophages fulfil in several important diseases of bovine species, including among the others tuberculosis and paratuberculosis, brucellosis or the disease related to peripartum, remain still partially elusive. The purpose of this review is to discuss the current knowledge of bovine monocytes and macrophages. We will describe methods for their purification and characterization of their major functions, including chemotaxis, phagocytosis and killing, oxidative burst, apoptosis and necrosis. An overview of the flow cytometry and morphological procedures, including cytology, histology and immunohistochemistry, that are currently utilized to describe monocyte and macrophage main populations and functions is presented as well.

Keywords:
monocytes; macrophages; innate immunity; bovine

1. Introduction: monocytes/macrophages and their main functions.

Monocytes are myeloid cells produced by the bone marrow that play pivotal roles in the immune response against infections and injuries. Monocytes and their corresponding tissue derivates, including macrophages and subpopulations of dendritic cells, are involved in almost all phases of the inflammation and bridge innate and specific immune responses [1]. In the bone marrow, hematopoietic stem cells differentiate to precursor cells. Pre-monocytic cells produce peripheral blood monocytes that transform into resident macrophages upon tissue entry [2]. Resident macrophages are among the first cell populations to sense a tissue pathogen or injury and generate the initial wave of cytokines and chemokines, alerting the immune system to incoming pathogens or tissue damage, skewing immune defences and activating and recruiting additional immune cells at the site of inflammation [2]. Functions of macrophages vary according to their location and type of activation. Alveolar macrophages are located in the lungs, and provide cellular defence against inhaled antigens, clearing the air spaces of infectious, toxic, or allergic particles that have evaded the mechanical defences of the respiratory tract [3,4]. In the brain, macrophages are identified as resident microglial cells and protect the Central Nervous System (CNS). Microglial macrophages play a pivotal role in synaptic pruning during development [5]. In a healthy status, microglia facilitate learning and memory and scavenge cellular or other debris. After CNS infections and injury, activated microglia fulfil the functions of resident macrophages during inflammation, recognizing pathogens or injured cells, activating phagocytic, antigen-presenting and cytokine/chemokine secretion functions. Activated microglia also contribute to the resolution of inflammation via switching to anti-inflammatory cytokine patterns, and promote intercellular matrix synthesis and angiogenesis.[6]. In the CNS, beside microglia, macrophages are also found in perivascular, meningeal and choroid plexus spaces, participating to the blood-brain barrier by modulating the entrance and the phenotype of immune cells during inflammation [7]. In lymph nodes, macrophages are classified as spinal or subcapsular sinusoidal, their main role being that of capturing antigens and presenting them to B cells [8]. The intestine provides one of the largest pool of macrophages in the body. Resident macrophages act as sentinels for pathogen recognition and elimination, maintaining the intestinal homeostasis by shaping host-microbiota symbiosis and regulating gut inflammation, promoting the crosstalking with T cells [9,10]. The splenic red pulp is a large tissue compartment containing macrophage lines able to perform several and diverse functions. The main role of splenic red pulp macrophages is to engulf senescent and altered erythrocytes, break down haemoglobin, recovering iron to the bone marrow, thus contributing to iron homeostasis [11] and to monitor, detect and phagocytize bloodborne pathogens. Other equally important functions of splenic red pulp macrophages include presenting

antigens to T lymphocytes of the splenic periarteriolar sheats [12]. In the liver, finally, resident macrophages are named Kupffer cells. In humans, Kupffer cells account for a large pool of tissue macrophages, and their main role is to remove toxins and pathogens [13].

Although the main role of macrophages is related to the protection against pathogens, they contribute to the resolution of inflammation by at least three ways: a) removing the pathologic stimulus by phagocytosis; b) producing anti-inflammatory cytokines, including for example TNF-α soluble receptor of IL1-R antagonist and c) removing leukocytes and necrotic debris in the inflammatory site. Macrophages carry out also tissue-repairing function and actively participate in the development of many autoimmune diseases development [1].

Peripheral blood (circulating) monocytes are cells with a consistent morphology (Fig. 1), and for many years they were regarded as a single functional population identified by the surface expression of the lipopolysaccharide receptor (CD14). However, the development of flow cytometry and multi-colour immunofluorescence, have allowed more detailed differentiation of monocytes, based on the additional expression of CD16 (FcγIIIR), the low-affinity receptor for the Fc regions of IgG [14]. According to CD14 and CD16 expression over the surface of the cells, at least two subpopulations of human monocytes: ($CD14^{++}$(bright)$CD16^{-}$and $CD14^{+}$(dim)$CD16^{+}$) have been identified. Further studies introduced, according with CD16 intensity of expression, other monocyte subpopulations, namely $CD14^{++}CD16^{+}$ and $CD14^{+}CD16^{++}$ [15]. Given their CD14 and CD16 membrane surface asset, circulating human blood monocytes can be divided into three different subpopulations [16]:

a) Classical monocytes (cM): "$CD14^{++}$ $CD16^{-}$ "cells providing approximately 90% of human blood monocytes.
b) Intermediate monocytes (intM): "$CD14^{++}$ $CD16^{+}$ cells" (approximately 10% of human blood monocytes)
c) Non-classical monocytes (ncM): "$CD14^{+}$ $CD16^{++}$" cells (in humans, a population with variable percentage).

Similar to humans, three monocyte subsets have been identified in bovine peripheral blood as well [17,18]. The heterogeneity and the functional differences between the three populations of bovine monocytes have been recently and extensively reviewed [19]. The authors compared bovine monocytes with their analogue human population, focusing on sub-type distribution and their main inflammatory functions, including adhesion and chemotaxis. Indeed, bovine monocyte specific functions (Table 1) have been studied in a relatively limited number of papers [18–20] and only partially resemble those of human counterparts.

Table 1

The inflammatory activity of bovine monocytes subsets				
Sub-type of monocytes	Relative percentage	Phagocytic capability [1]	ROS production[2]	Inflammasome activation
Classical monocytes (cM) $CD14^{++}CD16^{-}$	89%	+++	++	++
Intermediate monocytes (intM) $CD14^{++}CD16^{-}$	5-10%	++	+++	+++
Non-classical monocytes (ncM) $CD14^{+}CD16^{++}$	5/10%	+	+	+

[1] Phagocytic capability is expressed as percentage of FITC-positive cells within viable monocytes [18]: +++ = 80%, ++ = 56%, + = 40%

[2] ROS production is expressed in Mean Fluorescence intensity (MFI). +++ = 30 x 10^3, ++ = 50 x 10^3, + = 5 x 10^3.

[3] IL1β production (pg/mL) after ATP and LPS stimulation. +++ 4000 pg/mL, ++1000 pg/mL, + negligible

Differences between macrophage activation patterns 1q1q2ubetween cattle and other species also exist. For example, stimulating bovine monocyte-derived macrophages with pro-inflammatory signals do not produce the same reactions as compared to human and murine macrophages [19,21]. In humans and rodents, several other macrophage categories have been reviewed [22], the most important of which are listed in Table 2. The presence of most of these sub-groups in bovine peripheral blood has yet to be demonstrated.

Table 2

Principal macrophage subcategories and phenotypes in human and rodents

Macrophages sub-group	Type of response	Activity	Reference
M1	Pro-inflammatory,	Facilitate immunity to remove foreign pathogens and tumour cells, mediate tissue damage induced by ROS, impair wound healing and tissue regeneration	[22,23]
M2	Anti-inflammatory		[24]
M2a		Tissue repair and wound healing	[25,26]
M2b		Stress oxidative, efferocytosis	[27]
M2c		Pro-fibrotic activity phagocytosis of apoptotic cells	
M2d		Tumour-associated macrophages, angiogenesis and cancer metastasis	[28]
M3	Pro-inflammatory	Switch between M2 to M1 response, anti-tumour effect	[29,30]
M4	Pro-inflammatory	Predominant in atherosclerotic lesions	[31]

		low phagocytosis capability, high tissue repair capability	
M17	Pro-inflammatory	Increased phagocytosis in the presence of oxidized LDL	[21,32]
Mreg	Anti-inflammatory	Produce high levels of nitric oxide, CD86 and MHC Class II, Intense activation and proliferation, of IL-10 producing T cells	[33]
Mox	No clear pro- or anti-inflammatory activity	Weak phagocytosis, proatherogenic Development in response to oxidative stress damage	[34,35]

The transcriptomic data also revealed differential gene transcription between the three major monocyte subclasses of genes involved in immune defences, providing the evidence that monocytes subsets express different transcriptomes [36]. Indeed, the functions related to $CD16^+$ have to be revised and probably attributed between intermediate and non-classical subsets [37,38]. A sequential development between the two subsets was suggested [39], based on the concept that macrophages adopt *in vivo* several functional phenotypes, depending on continuous changes of the tissues' microenvironments. Given this background, M1/M2 and other subgroups are therefore not definite subsets but may represent the extremes of a continuum of different functional states [40].

2. Purification of bovine monocytes from blood: sorting or adherence

Normal blood values for monocytes in cows range from 25 to 840 cells/μL (average 400 cells/μL) and changes with age [41]. Purification of bovine monocytes starts from the collection of peripheral blood from the jugular or coccygeal veins, using a sterile Vacutainer™ blood collection vial containing EDTA (Becton Dickinson, USA). When a large amount of blood is needed (e.g. more than 200 μL) the use of blood bags containing citrate phosphate dextrose (Terumo, Japan) is preferred as a less stressful procedure for the animal. Blood collection must be as fast as possible for welfare issues and because the production of glucocorticoids associated with prolonged containment can profoundly affect *in vitro* monocyte activities. Although published several years ago, the paper by Godderies and co-workers [42] still provides a very good background for monocyte purification from bovine blood, specifically for the techniques related to adherence to glass or plastic wares. In general, methods to purify monocytes can be divided into two groups: those related to the adhesive capability of monocytes and those related to monocyte sorting by magnetic-activated cell sorting (MACS, Miltenyi Biotec, Germany).

The purification procedure based on the adhesiveness to tissues has been previously described by the team of Godderies and coworkers [42], whereas the procedure for the monocyte sorting by MACS

technique has been first described by Ceciliani et al. [43]. Figure 2 presents the morphology of cultured monocytes following MACS purification technique after 1, 2 and 4 days of culture. The first steps of purification are similar for both methods. Blood is collected into tubes (or bags) containing anticoagulant and processed within 1 hour of collection. Blood is centrifuged at 1260 × g for 30 min at RT to obtain the buffy coat. Mononuclear cells are recovered after dilution of the buffy coat 1:2.5 (v/v) in PBS/2mM EDTA, and 30 ml of this solution is overlaid on 15 ml Ficoll 1077 (Amersham Biosciences) and centrifuged for 30 min at 1500 × g at 4 °C. Mononuclear cells (i.e. monocytes and lymphocytes) are collected from the interface, also called mononuclear ring. The cells are resuspended in 50 ml PBS/2 mM EDTA and centrifuged for 7 min at 400 × g at 4 °C to remove platelets. To avoid non-specific activation of monocytes, it is pivotal to remove as many platelets as possible from the mononuclear cell fraction by performing second centrifugation in a 4% to 20% sucrose gradient layered over Ficoll-Paque PLUS (Sigma-Aldrich, USA). This procedure will effectively remove any platelet contamination [45,46]. Alternatively, consecutive centrifugations at low speed (400 x g for bovine monocytes), considerably reduces the number of platelets, that remains in the supernatant [43]. Table 3 summarizes the two protocols.

Table 3.

Purification methods for bovine monocytes *

Methods	Protocol
Adherence	A. **Polystyrene surfaces** 1. Isolated PBMCs are cultured in 75 cm^2 polystyrene culture flasks and incubated for 2 h at 38°C. 2. No-adherent cells are removed by pipetting out the supernatant and rinsing the flask with warm medium (38°C). 3. Adherent cells (monocytes) are detached by incubating them with Hank's Balanced Salt Solution (HBSS) without Ca^{2+} and Mg^{2+}, containing a mixture of 0.5 mg/mL Trypsin + 0.6 mM EDTA for 10 min at 23°C. 4. Cells are pelleted and washed (10 min 180 x g, 4°C) with unsupplemented RPMI 1640 medium, and finally resuspended in the culture medium. 5. After detaching monocytes from polystyrene flasks, to avoid monocytes loss by the binding to polystyrene, all procedures should be carried out at 4°C in polycarbonate conical tubes. **B. Plasma coated gelatin surfaces** 1. PBMCs are cultured in 75 cm^2 plasma coated gelatin (2%) culture flasks and incubated for 1 h at 38°C. 2. No-adherent cells are aspirated, and the flask rinsed with culture medium (38°C). 3. Adherent cells are detached by incubating the cells with HBSS without Ca^{2+} and Mg^{2+}, containing 10 mM EDTA for 5 min at 23°C. 4. Flasks are gently shaken, and cells recover with pipette and pelleted. 5. Cells are washed and resuspended in culture medium at 4°C.

Sorting	1. Monocytes are isolated from PBMCs with magnetic-activated cellular sorting technique, using a monocyte-specific monoclonal antibody ($CD14^+$). 2. PBMCs are incubated with anti-human CD14 labelled superparamagnetic beads (Miltenyi-Biotech) for 15 min at 4°C. 3. Cells are separated through magnetic separation using Macs column (Miltenyi-Biotech), by first eluting the cells not bound to the column ($CD14^-$) and then $CD14^+$ cells by removing the column from the magnet. 4. The purity of sorted cells is evaluated by flow cytometry.

The aforementioned techniques have both advantages and disadvantages that must be considered when choosing the adequate isolation method according to each experimental requirement. MACS technique is based on the immunomagnetic separation of the cells, which allows the specific isolation of a subset of monocytes of interest (e.g., $CD14^+$ fraction) with higher purity (> 98%) [43] than with the adherence based method [44]. Such specific marker separation is not possible when working on the isolation of monocytes by adherence from PMBC, where the authors often report the cells only as adherent (monocytes) and non-adherent (lymphocytes) [42]. Despite its advantages, this immune-based method also presents some disadvantages such as higher costs and the unavailability of antibodies used for the separation of monocytes of other species than humans. This issue can be addressed by purifying cells with the adherence-based method. Finally, the latter method is also cheaper and simpler, as no complex equipment is needed. The main disadvantage of the adherence method is the potential presence of other cellular population, such as eosinophils. When blood is collected from animals with a high concentration of eosinophils, the first step of purification, e.g. centrifugation over Ficoll layer, cannot entirely remove eosinophils, which in turn can contaminate monocyte population.

Once purified, population purity is assessed through flow-cytometric techniques.

Briefly, a total of 100 µL of cell suspensions are labelled with FITC-anti-CD14 antibody (clone TÜK4) and incubated in the dark for 15 minutes. Cells are washed twice and resuspended in PBS for flow cytometry. Fig. 3 shows representative flow cytometry dot plots of $CD14^+$ cells before and after MACS purification. The recovery of cells from either method yields an amount of homogenous monocyte population ranging from 8 to 10 millions of cells, starting from an initial blood volume of 200 mL.

Flow cytometric analysis shows that after MACS sorting, an enrichment of $CD14^+$ monocytes population > of 95% is obtained.

3. **Monocyte apoptosis, pyroptosis and necrosis (necroptosis)**

In multicellular organisms, a balance between cell proliferation and cell death is maintained to assure homeostasis [47]. Cells that are useless or superfluous, aged, damaged, and/or potentially harmful are selectively eliminated using genetically encoded mechanisms [48]. Up to now several types of cell death have been described: apoptosis, necrosis, both accidental and programmed (necroptosis), pyroptosis, cell death associated with autophagy, ferroptosis, netosis, among others [49]. However, apoptosis and necrosis are the best-characterized cell death ways so far. A comprehensive list of different cell death mechanisms has been recently published by the Nomenclature Committee on Cell Death [48].

Apoptosis is an ATP-dependent type of programmed cell death, generally characterized by distinctive morphological and biochemical changes. The morphological features of apoptosis include reduction of cellular volume, condensation of the chromatin, nucleus fragmentation, plasma membrane blebbing, maintenance of plasma membrane integrity until late stages and formation of apoptotic bodies followed by dead cells phagocytosis [50]. Cells undergoing apoptosis also show biochemical changes such as externalization of phosphatidylserine on the outer plasma membrane [51], the release of mitochondrial intermembrane space proteins (Cytochrome C, Smac/DIABLO) [52], DNA fragmentation and caspase-dependent activation [53]. Several of these features were exploited to measure apoptosis rate. Apoptosis is generally not associated with inflammation, due to the absence of cells' contents release, resulting in cell clearance from the body with minimal damage to the surrounding tissues [54].

Understanding the monocyte cell death mechanism(s) is important, as the way of cell death (necrosis *vs.* apoptosis *vs.* pyroptosis) can influence the pro- and anti-inflammatory responses [55] and therefore interfere with the proper resolution of inflammation, or the clearance of the inflammatory focus from the pathogens, or cancer development [56]. Moreover, apoptosis rate is critical for normal cell turnover and proper development and functioning of the immune system. Indeed, apoptosis provides a way to control the activity of blood monocytes, by increasing or reducing their abundance in the inflammatory environment.

In contrast, necrosis is generally described as an "accidental or uncontrolled" way of cell death caused by extreme physical or chemical stress [57]. The rapid cytoplasmic granulation/vacuolization, cellular and organelles' swelling in necrotic cells, results in plasma membrane rupture, organelle breakdown, intracellular content spillage, inflammation and surrounding tissue damage [47,54]. Nevertheless, it is now known that necrosis can also occur as a caspase-independent form of regulated cell death, also known as necroptosis, following many defined steps and signalling events, just like apoptosis [57].

Necrosis is the term currently used for nonapoptotic death and has been characterized as passive, accidental cell death resulting from environmental perturbations with the uncontrolled release of

inflammatory cellular contents. The presence of necrosis provides evidence that a cell has died, but not necessarily how the death occurred. The necroptosis is defined as the caspase-independent, regulated cell death (RCD). In the recent years, research studies concerning caspase-independent, non-apoptotic forms of programmed cell death (PCD) have enabled the identification of backup mechanisms to allow the cells to undergo suicide or RCD under conditions where the caspase machinery is defective or inhibited [58].

Another type of regulated necrosis so far described and measured in monocytes and macrophages is pyroptosis. Pyroptosis occurs in response to microbial products or other intracellular perturbations, which cause the production of proinflammatory cytokines like IL-1β, leading to cell swelling and death [57]. Being initially thought to occur only in macrophages and leukocytes during inflammatory conditions, pyroptosis has now been observed in several other cell types, including fibroblasts and endothelial cells [59]. Pyroptosis is generally characterized morphologically by membrane pore formation, cell swelling, membrane disruption and DNA damage, whereas biochemically by an inflammatory caspase activation (non-apoptotic caspase-1), that mediates cytokine maturation [57,60]. The identification of distinctive and specific markers in all of these three types of cell death has long been used for their *in vitro* and *in vivo* discrimination in many cell types including monocytes and macrophages.

3.1. In vitro assays measuring monocytes/macrophages apoptosis

In vitro apoptosis can be determined through several methods: by characterizing cell morphology through microscopy or by measuring biochemical cell death features, like caspase activation, that is activated uniquely during the apoptosis [47]. Methods relying on flow cytometry have also been widely applied in human and murine research to distinguish apoptosis from necrosis [61].

Specifically, the measurement of the activity of the two main effectors enzymes in apoptosis, namely caspase-3 and -7, has been already reported and validated in bovine monocytes ($CD14^+$) [20,32]. In these studies, the activation of the two enzymes was measured through fluorometry, using a detection assay that contains aa pro-fluorescent substrate the rhodamine 110, bis-(N-CBZ-L-aspartyl-L-gluta-myl-L-valyl-L-aspartic acid amide - Z-DEVD-R110) and a cell lysis buffer that supports optimal caspase activity. The assay is adapted to small well formats, such as 96 or 384-well plates. Depending on the selected format, between $5x10^4$ cells for 384-well up to $1x10^5$ cells for 96-well plates are seeded in final volumes of 25 μL to 50 μL, respectively [43,63]. In a second step, an equal volume of Apo-ONE^{TM} Homogeneous Caspase 3/7 Reagent (Promega, USA), containing the pro-fluorescent substrate and previously diluted 1:100 in the reaction buffer, is added to each well. Plates are then

incubated in a plate shaker at 300 rpm for 1 h at room temperature. According to the manufacturer's instructions, incubation times should be optimized for each model as minimal apoptotic induction and low cell numbers may require extended incubation periods. Finally, upon cleavage of the DEVD peptides by caspase-3 and -7 activities, the fluorescent compound rhodamine 110 is released and fluorescence intensity can be measured using a fluorescence plate reader (excitation at 485 nm, emission at 530 nm).

Caspase activity can also be measured through colourimetric assays. For example, a caspase colourimetric protease assay (Aportaget; Invitrogen, Canada) kit has been used to determine the activity of caspases-3, -6, and -9 in monocytes infected with *Mycobacterium bovis* [64]. This assay can be carried out by lysing a pellet of infected monocytes containing 5×10^6 cells with 50 μL of chilled cell lysis buffer provided by the kit and incubated for 10 min, before centrifuging them at 10,000 × *g*. The supernatant containing the cytosolic fraction is transferred to a fresh tube and the protein concentration is quantified. After having adjusted the cytosolic fraction concentration (200 μg/mL) in the cell lysis buffer provided in the kit, 50 μL of it are transferred to 96-well round-plates and 50 μL of 2×kit reaction buffer, containing 10 mM of dithiothreitol (DTT) and 200 μM the respective substrate for the caspases, is added in a volume of 5 μL. Finally, samples are incubated at 37°C for 2 h in the dark and then read at 405 nm with a 490-nm reference filter in a microplate reader. Bovine monocyte-derived macrophages apoptosis has also been detected trough fluorometric analysis of caspase-3 activity [63] and relative quantification of histone-complexed DNA fragments, that are often out of the cytoplasm of cells undergoing apoptosis [65], using Cell Death Detection ELISAPLUS kit (Roche, Switzerland) [66]. Because histone-complexed DNA release is not an exclusive phenomenon of apoptosis but also can occur in necrotic cells, using complementary assays is preferred [67].

3.2. In vitro assays measuring monocytes necrosis

The permeabilization of cells' plasma membranes and its consequent release of cellular content are some of the hallmarks of necrosis. The release of lactate dehydrogenase (LDH), an ubiquitous cytosolic enzyme, into the supernatant after membrane integrity loss has long been measured to detect necrosis in multiple cell types by spectrophotometry, including bovine monocyte-derived macrophages [63,66,68]. Specifically, in the study of Denis and coworkers [66], a commercially available kit (CytoTox 96®, Promega, USA) was used to measure the LDH released to the supernatants by a 30-minute coupled enzymatic assay that leads to the conversion of a tetrazolium salt (iodonitro-tetrazolium violet; INT) into a red formazan product, which is proportional to the

amount of LDH present and thus to the number of damaged cells. Besides INT, the kit reagents also contain the substrates lactate, NAD^+ and diaphorase to complete the reaction, as the first two are needed to produced reduced nicotinamide adenine dinucleotide (NADH) that is later used to convert INT into the coloured product in the presence of diaphorase [68]. According to the manufacturer instructions, cells are first seeded in 96- or 384-well plates and treated with the desired experimental design. Afterwards, the supernatants are transferred to a fresh plate (50 μL for a 96-well and 12.5 μL for a 384-well plate) and an equal volume of CytoTox 96® Reagent is added. Plates are protected from light and incubated for 30 min at room temperature. Finally, 50 or 12.5 μL of Stop Solution are added and absorbance measured 490nm or 492nm [66]. Other techniques based on differential uptake of DNA binding dyes, like propidium iodide (PI), that do not enter living cells, have also been used for determination of bovine necrotic neutrophils [69], blood monocytes and macrophages ($CD14^+$) isolated from the mammary gland through flow cytometry [70].

3.3.In vitro assays measuring monocytes pyroptosis

The discrimination between necrosis and pyroptosis can be a challenging task as many of the hallmarks for regulated necrosis such as plasma membrane rupture, cytoplasmic granulation/vacuolization and cellular/organelle swelling are also shared by pyroptosis [71]. The measurement of LDH release has also been implemented for pyroptosis determination of human and murine bone marrow-derived macrophages, as it is a simple and cost-effective technique [62,72]. DiPeso and coworkers monitored the cells' LDH secretion, as previously described [59,73], after reacting with a pyroptosis inducer called RodTox that activates the NAIP2/NLRC4 inflammasome, leading to caspase-1 activation and pyroptosis. Additionally, a more specific way to measure pyroptotic death of individual cells *in vitro* can be carried out through the measurement of caspase-1 activation and inflammasome formation (NLRP3) by both fluorescence or confocal microscopy [74]. Cells are labelled with the caspase-1 activity probe FAM-YVAD-FMK that specifically binds to the caspase-1 family proteases, and with antibodies against inflammasome components such as the adaptor protein ASC that recruits pro-caspase-1. For that, murine marrow-derived macrophages are first seeded in 96-well plates and stimulated with 100 ng/mL of LPS for 3 h at 37°C to prime Toll-Like Receptor 4 (TLR4), the first step needed for NLRP3 activation. Afterwards, the medium is removed, and cells are stimulated with fresh DMEM medium-containing 5 μM nigericin to induce the second step for the activation of the NLRP3 inflammasome, and 5 mM glycine to reduce the cell lysis caused during caspase-1 activation. Cells are then incubated for 60 min at 37°C and 5% CO_2, and during the last 45 min incubated as well with 30x of the FAM-YVAD-FMK probe, which is

prepared according to the manufacturer's instructions. After incubation, the medium is removed and the cells are washed three times for 5 min with cold PBS. Finally, the cells are fixed and stained with a fluorescent nucleic acid stain to label the nuclei and mounted for a correct visualization by confocal microscopy, with an excitation/emission of 492/520nm for the FAM-YVAD-FMK probe. For the antibody staining of the inflammasome component (ASC), after seeding, priming and exposing the cells to nigericin, the cells are washed with cold PBS, fixed and permeabilized on ice and in dark for 30 min. Macrophages are washed with the washing buffer and the primary antibody anti-ASC (1:500) is added and cells are incubated for 1 h on ice. The cells are again washed and the secondary antibody (fluorescent dye conjugated goat anti-mouse; 1:500) is added for another 1 h on ice. During the last 5 min of this incubation, the dye to stain the cells' nuclei is also added. Finally, cells are washed and prepared for confocal analysis with an excitation/emission for the secondary antibody of 555/580 nm. According to Hartigh and Fink, to successfully determine pyroptotic cells the nuclear morphology should be considered, as cells with active caspase-1 possess a rounded and condensed nuclei without visible nucleoli, often present in cells without caspase-1 activation [74].

Even though the previously described techniques have been carried out mostly in human and murine macrophage models, the same ones can be applied to bovine monocytes/macrophages' pyroptosis determination, although they have been not tested so far.

3.4. Flow cytometric assays to evaluate apoptosis, necrosis (necroptosis) and pyroptosis

Determining the number of dead cells during a flow cytometry study is a prerequisite to obtain reliable data, given that dead cells can bind in a non-specific way to many reagents. Therefore, removing dead cells from flow cytometry data is a prerequisite and a critical step to ensure accurate results and analysis [55]. A widely used flow cytometric assay to define cell viability is based on the reaction of a fluorescent dye, such for example propidium iodide (PI), with cellular amines. This die cannot penetrate live cell membranes: consequently, only cell surface proteins are available to react with the dye, resulting in dim staining. The reactive dye can permeate the damaged membranes of dead cells and stain both the interior and exteriors amines, resulting in more intense staining [72]. In normal living cells, the phosphatidylserine (PS) is located at the side of the cytoplasmic surface of the cell membrane. However, during early apoptosis, PS is translocated from the cytosolic side of the intact plasma membrane to the extracellular surface. Early apoptotic cells cannot, therefore, be reliably identified using approaches that are based on membrane permeability. Annexin V is a protein with high affinity, specificity, and sensitivity for PS. Thus, the binding of annexin V to cells can be used

as a marker of early apoptosis [75] and provides the most commonly used approach for determining apoptosis [55].

A typical experimental protocol to detect apoptosis is the following: 100 μL of cells suspension ($1x10^6$ cells/mL) in 1X annexin-binding buffer are incubated with 5 μL of fluorescein isothiocyanate (FITC) annexin V and 1 μL of PC5.5-PI (100μg/mL) in the dark at room temperature for 15 min. Finally, 400 μL of the annexin V binding buffer is added and the cells are analyzed by flow cytometry. The binding of annexin V to PS is reversible, and so samples must be analyzed as soon as possible and no later than 1 h after labelling. Fig. 4 illustrates the typical aspect of a dot plot flow cytometry analysis using annexin V/PI double staining to determine in the percentages of live, apoptotic and necrotic bovine peripheral blood lymphocytes and monocytes. Beside annexin V staining, the measurement of caspases activity is also widely used to determine the apoptosis rate. Caspases are a family of cysteine proteases that plays a key role in apoptosis and inflammation. These enzymes are present in healthy cells as inactive zymogens, but when stimulated they undergo autolytic cleavage to become fully active. Consequently, many of the cleaved fragments remain intact during apoptosis and can be detected using specific antibodies. These antibodies can be used to specifically label cells in which caspase cleavage has occurred, allowing to quantify these cells by flow cytometry. Several antibodies that specifically recognize caspase-cleaved fragments have been generated, including antibodies that recognize the cleaved form of caspase-3, a key protease activated during the early stage of apoptosis [76].

For flow cytometric detection of active caspase3, $1x10^6$ cells are washed with PBS and then resuspended with 100 μL of fixation/permeabilization buffer (Cytofix/Cytoperm™, BD Biosciences, USA)) for 20 min at room temperature. In the following step, cells are washed twice with 600 μL of erm/Wash™ (BD Biosciences, USA) buffer and stained with the PE- rabbit anti-active caspase-3 antibody (clone C92-605) for 40 min at 4°C. Cells are then washed and resuspended in Perm/Wash™ buffer for flow cytometric analysis.

Both pyroptosis and apoptosis are programmed cell death mechanisms but are dependent on different caspases. Pyroptosis is triggered by caspase-1 after its activation by various inflammasomes and results in lysis of the affected cell. Pyroptotic cell death could be assessed in PBMC and monocytes by flow cytometry by measuring the double-positive staining of activated caspase-1 and PI [77]. Furthermore, Hussen and coworkers [20], analyzed the inflammasome activation in bovine monocytes through the evaluation of caspase-1 activation. Authors used the FLICACaspase-1 detection KIT (Thermo-Fisher, USA), a fluorescent inhibitor of active caspase-1 (FAM-YVAD-FMK), which binds activated caspase-1. First, bovine PBMC or purified monocytes ($1 x10^6$) are stimulated for 2 h with LPS (100 ng/mL). Then ATP (2 mmol/L) is added to the cell culture for a

395 further 30 min. After stimulation, cells are detached from the plates by Accutase™ (Sigma-Aldrich,
396 USA) treatment (incubation for 15 min at 37°C and 5% CO_2). Cells are then suspended in 300 μL
397 RPMI medium and 10 μL of the 30X FLICA solution is added. After the incubation (1 h at 37°C and
398 5% CO_2) with FLICA, cells were washed two times with the FLICA buffer and suspended in 200 μL
399 of the same buffer. For flow cytometric analysis PI (2 μg/mL final concentration) is added to exclude
400 dead cells.
401
402 4. **Monocyte and macrophage chemotaxis**
403
404 Chemotaxis is the ability of cells to migrate in response to a chemical signal or chemoattractant
405 gradient concentration. It is a crucial function of leukocytes, including monocytes, as they fulfil their
406 defensive functions by migrating from blood to affected tissues, where they produce pro-
407 inflammatory cytokines and reactive oxygen species (ROS) and eventually phagocyte and destroy the
408 invading pathogens [78].
409 Monocyte chemotaxis is determined by using the Boyden chamber assay, composed of an upper and
410 a lower compartment separated by a porous membrane (Fig. 5a). This assay consists mainly of
411 monitoring the migration of the cells through a microporous membrane. In general, the cells are
412 seeded in the medium-filled upper compartment and are allowed to migrate through the pores of the
413 membrane, towards the medium-filled lower compartment where chemoattractants are present [79].
414 To assure the correct migration of the cells through the membrane, this one must be selected with the
415 appropriate pore size for the cells of interest. Human monocyte chemotaxis is usually triggered by N-
416 Formylmethionine-leucyl-phenylalanine (N-fLMP), a formylated peptide derived from bacteria [80],
417 which specifically reacts with Formyl Peptide Receptors [81]. Bovine cells do not have N-fLMP
418 receptors [82,83]. In this species, therefore, chemotaxis should be triggered with other
419 chemoattractants, including, such as, for example, zymosan activated serum (ZAS) [84]. The *in vitro*
420 chemotactic capacity of bovine monocytes has been determined using this principle with a modified
421 Boyden chamber [84]. In this study, bovine monocyte migration was measured using a 48-well
422 microchamber, where the chemoattractant ZAS was added in the lower part of the chamber. A PVP-
423 free polycarbonate filter (5 μm pore size) was layered onto the lower wells and covered with a silicone
424 gasket and finally with the top plate above. In the upper wells, 1.5 x 10^6 cells/mL were seeded (50 μL
425 final volume) and the chamber was incubated at 37°C in 5% CO_2 for 105 min. The microchamber
426 was disassembled and the filters were removed carefully, the non-migrated cells on the upper part of
427 the filter were removed by scraping and the migrated cells found in the lower part of it were stained

with Romanowsky type stains including May-Grünwald-Giemsa and Wright's stains. Finally, cells were counted in different high-power oil-immersion fields.

Modified Boyden chamber devices, allowing a more convenient and user-friendly methodology to carry out the cell migration studies, are commercially available. Such is the case of the transwell migration plates (Fig. 5b), that contain easy-to-use permeable cell culture membrane inserts of different pore sizes that can be removed from the plates when needed to stain and count the cells that have migrated through the membrane. The transwell migration assay has been described to assess the chemotactic activity of human blood monocytes and the human monocyte cell line THP-1 [85] and can be also used for bovine studies. In this study, $1x10^5$ of THP-1 and blood monocytes were seeded in the upper chamber of a 24-well transwell migration plate in a final volume of 125 µL of serum-free media. The monocyte chemoattractant protein-1 (MCP-1) and "platelet-releasate", which is the content released by secretory granules of activated platelets, were added as chemoattractants to the lower chamber in a final volume of 1 mL and plates incubated for 2 h at 37°C. After incubation, the upper chambers were removed and placed into 2.5% glyceraldehyde for 15 min to fix the migrated cells found on the underside of the membrane. The membranes were washed with PBS, and the upper chambers were stained with 0.1% of crystal-violet for 45 min. Finally, cells were washed twice with PBS and cells in ten 40x fields were counted using light microscopy.

Chemotaxis of monocyte-derived macrophages has been measured as well [86], using the same technique, e.g. the migration through Boyden chamber, previously described.

The Boyden chamber technique has been modified over the years to allow the quantification of total migrating leukocytes concurrently with the determination of their phenotype to associate specific inflammatory responses with distinct leukocyte subsets. Gomez-Lopez and coworkers [87] validated in humans a combined Boyden-flow cytometry chemotaxis assay (CBFCA), that allows the accurate quantification and recovery of the migrating leukocytes for subsequent phenotyping and characterization in a single assay, facilitating the understanding of leukocyte trafficking during the inflammatory response. The combined chemotaxis assay is performed under the same conditions described for the classic method, but only the polycarbonate membrane was used. Following incubation, the leukocyte suspension in the lower well is recovered and cells counted by flow cytometry. To our knowledge, the CBFCA assay has not yet been applied to study chemotaxis of bovine monocytes.

5. Monocyte/macrophages phagocytosis and killing

Phagocytosis and respiratory burst are two of the most important functions for monocytes/macrophages and polymorphonuclear cells and are essential for both the elimination of invading microorganisms and the presentation of antigens to T-cells. Phagocytosis is a process in which target particles are engulfed and taken up by other cells, crucial to the innate immune response and consequently regulating the adaptive immune response [88]. Phagocytic affinity is related to particular marker expression patterns, directed by a complex range of cell surface receptors, and may also change in different populations of monocytes [88]. Bovine monocytes mediate the inflammatory response activated in phagocytosis and killing capability, which leads to different abilities to phagocytose bacteria between the different monocyte's subsets – cM are the ones with the highest phagocytosis, followed by intM and ncM with the lowest ability [18]. The phagocytosis ability of monocytes can also relate to other factors such as age, breed, nutrition and the clinical status of the animal [89–91]. Lymphocytes in neonatal calves have poorer phagocytosis ability but counterbalance with higher absolute numbers, in contrast to monocytes of neonatal calves that showed a higher bacterial uptake than 3-9 week old calves, suggesting that the monocytes contribute to the compensation of impaired earlier innate immune defence in infancy [92]. A similar mechanism seems to take place in the mammary gland, where a greater number of viable macrophages may partially compensate for the functional deficit in polymorphonuclear cells in cows with high somatic cell counts [93].

The *in vitro* phagocytosis assay of bovine monocytes can be performed by co-culturing the cells with opsonised fluorescein-labelled bacteria and then incubating them at 37^{o}C in a humidified atmosphere of 5% CO_2 for 1 h. The cells are washed twice with sterile HBSS and then incubated with trypan blue to quench non-internalised fluorescent bacteria, and after two subsequential washes with HBSS, the intensity of the fluorescence, which can be correlated with the phagocytic ability, can be measured [44]. Improved results have been achieved *in vitro* in the study of monocyte-derived macrophages phagocytosis when opsonizing bacteria with naive-autologous sera than bacteria opsonized with fetal bovine serum [94].

Phagocytosis assays of monocyte-derived macrophages can also be performed by co-incubating the cells with opsonised bacteria in a ratio of one bacterium to one macrophage, in a water bath at 37^{o} C under continuous rotation. The suspension is removed and added to ice-cold gelatine-Hanks' salt solution to stop phagocytosis, and the macrophages are centrifuged (110 x *g* for 4 min) to remove the non-ingested bacteria, that remain in suspension in the supernatant fluid. The supernatant is then seeded on tryptic soy agar plates, in dilutions between 10 and 100 colony counts, incubated in 8% CO_2 at 37^{o}C for 72 hours. The results are expressed as the percentage of survival of non-phagocytized/non-cell-associated bacteria based on the formula [94]:

$$Percent\ survival = \frac{CFU\ of\ bacteria\ after\ incubating\ for\ 120\ min}{CFU\ of\ bacteria\ at\ time\ 0}\ x\ 100$$

The monocyte's and macrophage's ability to bind, internalize and kill bacteria occur as independent and sequential steps, and, as a result, a phagocyte may be able to ingest a pathogen and yet not manage to kill it. Thus, the phagocytosing and killing capabilities of monocytes and macrophages should be measured by separate assays [95]. The *in vitro* intracellular bacterial killing assay is performed by co-incubating bovine monocytes (5 x 10^5 cells) with opsonised bacteria (*E. coli*) for 60 min. The unbound bacteria are removed, by centrifuging them at 110 x *g* for 5 min, and the cell pellet is resuspended in HBSS with 100 µg/mL gentamicin, to kill any remaining extracellular bacteria, and then incubated for 1 h at 37º C. Cells are washed with warm HBSS and then centrifuged again at 110 x *g* for 5 min to remove the gentamicin. The cells are then lysed by incubation on ice with 0.5% Triton X-100 for 10 min and the surviving bacteria are seeded on MacConkey agar plates for CFU counting [44].

Flow cytometric assays have been developed to quantify phagocytosis and respiratory burst in whole blood, as well as isolated cells from blood, tissue or secretions [96,97]. Hussen and coworkers [98] reported a flow cytometric assay to evaluate phagocytosis capacity of bovine monocytes. FITC-conjugated and heat-killed *S. aureus* or *E. coli* were opsonized with heterologous bovine serum (diluted 1:10 with PBS) for 45 minutes at 37°C. MACS-separated bovine monocyte subsets were incubated for 24 h (37°C, 5% CO_2) in RPMI medium. After this resting period, cells were incubated with opsonized bacteria (50 bacteria/cell) for 40 minutes (37°C, 5% CO_2). Control samples were incubated without bacteria. After incubation, samples were analyzed using flow-cytometry after the addition of propidium iodide (2 mg/mL final concentration) to exclude dead cells. Phagocytic activity of different monocyte subsets is defined as the percentage of green fluorescing cells among viable cells.

6. Monocyte/macrophages ROS production

Generation of reactive oxygen species (ROS) is a critical factor in the antimicrobial activities of monocytes, though it may also lead to cellular cytotoxicity and/or tissue damage. The intracellular presence of ROS can result in damage to the intracellular constituents and oxidative stress, which may have consequential alterations in monocyte's function [88]. As other functional abilities, ROS production differ between different monocyte populations – bovine intM is reported to present the

strongest production between the subsets [18] – and virulent pathogens of cattle, such as *N. caninum*, may also regulate ROS production of infected macrophages [88].

The production of oxidative burst activity of bovine monocytes can be measured *in vitro* using a cytochrome C reduction assay, as similarly used in bovine and caprine neutrophils and goat monocytes [99,100]. The measurement of cytochrome C reduction is commonly used for the measurement of extracellular superoxide anion [101] and demonstrated a dose-dependent specificity in detecting extracellular superoxide production in bovine neutrophils [99]. The extracellular ROS production is measured by mixing 2 x 10^5 monocytes in RPMI-1640 medium (adjusted final volume on wells of 200 μL) and cytochrome C (1 mM). Parallel studies to assess the ROS production after inducing a pro-inflammatory challenge to the cells, by adding phorbol 12-myristate-13-acetate (PMA), can also be performed. PMA (2.5 μg/mL final concentration) and cytochrome C (1 mM) are added to the cells and the absorbance is measured immediately with a plate reader every 30 min for 2 h at a wavelength of 550 nm. Background values are measured from wells with cytochrome C diluted in RPMI-1640 and subtracted from all values [102]. Analysis of ROS generation via cytochrome C reduction assay has been used in bovine monocytes and alveolar macrophages (AM), revealing that monocytes appear to be less responsive in ROS formation than AM, likely for being more immature and thus possessing less cytoplasmic organelles enabling metabolic processes [103]. Production of ROS reduces substrates such as dichloro-dihydro-fluorescein-diacetate (DCHF) or dihydro-rhodamine 123 (DHR 123) that become fluorescent and can be quantified by flow cytometry. Hussen and Coworkers [98] reported a typical flow cytometric analysis of ROS generation on bovine monocyte. The analysis is performed after stimulation of cells with PMA (50 nmol/L) or heat-killed and serum opsonized *E. coli* (50 bacteria/cell) for 15 min (37°C, 5% CO_2) in the presence of the fluorogenic substrate DHR 123 (750 ng/mL). ROS generation is calculated as Mean Fluorescence Intensity (MFI) of gated monocyte region after subtracting the MFI of non-stimulated cells.

7. Monocyte/macrophages production of cytokines

Cytokines are important chemical messengers produced by both innate and adaptive immune cells, that allow the communication between both types of immunity and within the adaptive immune system [104]. Specifically, monocytes and macrophages play a critical role in immune regulation by producing a wide range of pro and anti-inflammatory cytokines like TNF-α, IL-1β, IL-6, IL-8, IL-10, IL-12, and TGF-β1 [105]. At the same time, these cytokines modulate their functions by stimulating or inhibiting their microbial activities in an autocrine and paracrine manner [106] and are also involved in cell migration, activation, proliferation and antibodies' production. Moreover,

monocytes and macrophages can be further classified into different subsets according to the cytokine profile they produce [107]. Therefore, the measurement of monocyte and macrophage cytokine production is a highly useful approach for phenotyping and characterizing their functionality.

Bovine monocytes' cytokine production can be measured mainly by two approaches: detection of secreted cytokines at the protein level through enzyme-linked immunoabsorbent assays (ELISAs) [64] or by measuring cytokines' mRNA abundance by real-time quantitative PCR (q-PCR) [16,21,62,108].

Several commercially available ELISA kits have been used for the quantification of bovine cytokines, including IFN-γ [109,110], TNF-α [111], IL-1β [112] and IL-4 [111]. However, the quantification of secreted cytokines in monocytes/macrophages can be performed by other methods. Recently, type 1 IFN was measured in ovine alveolar macrophages' supernatant by using an IFN bioassay [113]. An IFN bioassay is a method to quantify IFN biological activity units, meaning it measures the actual biological power of an IFN preparation in a specific cell line or biological system [114]. It is well known that IFNs types' cytokines induce a potent antiviral activity in vertebrate cells [115]. Therefore, this method mainly relies on type 1 IFN antiviral properties and determines the amount of IFN in a solution- usually secreted by virus-infected monocytes/macrophages- according to its ability to neutralize viral replication and protect the infected cells in culture from cytopathic effects. One of the most common IFN bioassays is based on the quantification of the fluorescence intensity of viral-encoded reporter proteins, like green fluorescent protein (GFP), during the virus replication in cell culture [116]. The protective effects of IFN are then quantified by measuring the fluorescence intensity and is determined by the ED50 that is the amount of IFN needed to reduce the fluorescence by 50% [114]. Briefly in ovine, the bioactivity of IFN secreted by Sendai virus-infected ovine alveolar macrophages was quantified by first serially diluting the IFN containing supernatant in DMEM medium supplemented with FBS and antibiotics. This supernatant was then added to 2×10^4 ovine fibroblasts that were seeded the day before in 96 well plates, and cells were incubated at 37 ◦C for 24 h. After incubation, supernatants were removed and ovine fibroblasts were infected with Recombinant Vesicular Stomatitis virus expressing GFP (VSV-GFP) at a multiplicity of infection of 0.01 and incubated at 37 ◦C. After 18 h post-infection, the green fluorescence of VSV-GFP infected cells was detected by using a plate reader with an excitation wavelength of 480 nm and emission of 518 nm [113]. This method gives extra information when compared to ELISA, as by quantifying IFN with a bioassay one can measure the antiviral activity on a specific experimental condition without needing absolute numbers [114].

To measure bovine monocytes' cytokines mRNA abundance using qPCR [62], RNA from at least 1 x 10^6 cells/well is extracted by using guanidinium-acid-phenol extraction methods, such as TRizol™

(Thermo-Fisher, USA) or Qiazol™ (Qiagen, Germany), or commercial kit [117]. After having assessed the quality and concentration of RNA using a NanoDrop ND-1000 UV–vis spectrophotometer, an Agilent Bioanalyzer or a Qubit fluorometer, genomic DNA is eliminated using DNase I, RNase free kit. Reverse transcription is then carried out on RNA using commercially available cDNA Synthesis kit. The cDNA is then used as a template to perform qPCR or microarray. To carry out a reliable relative quantification, at least three adequate reference genes should be identified and the geometric mean is used for normalization [118,119]. In the published MIQE (Minimum Information for publication of Quantitative real-time PCR Experiments) guidelines is indeed proposed the validation of RGs for all qPCR experiments [120]. Statistical softwares like geNorm™, NormFinder© and BestKeeper can be used to assess the appropriateness and stability of these genes [121–124]. The list of reference genes that have been used for quantitative real-time RT-PCR gene expression studies in monocytes and macrophages is reported in Table 4.

Table 4.

Validated reference genes for monocytes and macrophages used for qPCR.

Symbol	Name	Accession number	Cell target	Target specie	Ref.
HMBS	Hydroxymethyl-bilane synthase	NM_013551	Macrophages	Murine	[121]
B2M	β-2-microglobulin	NM_009735			
ACTB	β-actin	NM_001101.3	THP-1 monocyte cell line	Human	[122]
RPL37A	Ribosomal protein L37a	NM_000998.4			
SF3A1	Splicing factor 3 subunit 1	NM 001081510	Monocytes/ Other tissues	Bovine	[123]
ACTB	β-actin	BT030480.1			
HMBS	Hydroxymethyl-bilane synthase	NM 001046207.1			
H3F3A	H3 histone, family 3A (H3-3B)	NM_001014389.2	Monocytes	Bovine	[62]
SF3A1	Splicing factor 3 subunit 1	NM 001081510			
YWHAZ	Tyrosine 3-monooxygenase/tryptophan 5-monooxygenase activation protein, zeta polypeptide	XM_025001429.1			

Additional studies have also reported the adequateness of some of the previously mentioned reference genes like YWHAZ and ACTB in different ovine tissues (brain, spleen, mesenteric lymph nodes) [125]; and of YWHAZ in goats' frozen whole blood [126], but not specifically in

615 monocytes/macrophages. Remarkably, the stability of all the genes tested in different ovine tissues
616 changed significantly within each tissue, suggesting that there is not a unique universal reference gene
617 for all tissues or cell types and that their stability must be evaluated prior the start of each study. Such
618 a statement can be further confirmed by the fact that in a previous study, ACTB was not an appropriate
619 reference gene for gene expression analyses in ovine interstitial cells[127].
620 Intracellular cytokine staining (ICS) of stimulated whole blood or isolated PBMC followed by flow
621 cytometric analysis is a well-established method for detecting cytokines production at the single-cell
622 level. Recent studies developed a cytokine flow cytometric assay to detect intracellular IFN-γ in cattle
623 naturally infected with *M. bovis* [128]. The detection of intracellular IFN-γ may represent an
624 important alternative approach for an improved method of detection of cattle secreting IFN-γ below
625 levels of detection in the culture medium.
626 It is important to consider that the analysis of intracellular targets using flow cytometry presents
627 several technical challenges that are not generally encountered in the measurement of cell surface
628 epitopes. In general, cells must be first fixed to preserve and maintain both the structure and location
629 of target epitopes, then permeabilized to allow antibodies access to all cellular compartments, such
630 as the cytoplasm. In general, cell fixation is accomplished using either crosslinking fixatives, such as
631 formaldehyde, or low molecular weight alcohols (methanol), which generally act to coagulate
632 proteins. However, the fixation–permeabilization and methanol treatment need to be validated for the
633 complete set of antibody conjugates used for a new experiment [55].
634 Short-term stimulation of PBMC (6-16 h) with antigen or peptide mixtures is required to induce
635 cellular activation and production of cytokines. Cells can also be stimulated in 15 mL conical
636 polypropylene tubes or plates. Secretion inhibitors such as Brefeldin A and/or Monensin are added at
637 the time of stimulation (for peptides) or after 2 h (for proteins) to allow secreted cytokines and other
638 proteins to be retained intracellularly. At the end of the stimulation period, cells can be held at 4–
639 18°C until ready to process. They are then co-incubated with 0.2 mg/mL of EDTA at room
640 temperature to remove adherent cells, fixed, permeabilized and stained for intracellular determinants.
641 In some cases, surface marker staining is carried out jointly with intracellular staining. However, most
642 other cell-surface markers require staining before fixation, because the epitopes recognized by
643 staining antibodies are sensitive to fixation and/or permeabilization reaction [129].
644
645 **8. Phenotypic characterization of monocyte subsets: the flow cytometry approach**
646
647 The flow cytofluorimetric approach allows the immunophenotypic characterization and absolute
648 count of the monocyte subsets. Hussen et al. [17] demonstrated for the first time that bovine

649 monocytes can be distinguished in three subsets on the differential expression of CD14 and CD16.
650 Similar to humans, bovine cM are $CD14^{+}CD16^{-}$ and intM $CD14^{+}CD16^{+}$. On the contrary, ncM are
651 $CD14^{-}CD16^{+}$. Further evidence [19,130,131] suggested that CD14 is not a useful marker for the
652 immunophenotyping studies and cell sorting experiments of non-classical monocytes.
653 CD172a, a member of signal regulatory protein (SIRP) family, is a marker for myeloid cells and
654 neurons [132]. Two specific mAbs (Table 5), can be successfully used to identified bovine
655 monocytes, granulocytes, macrophages and dendritic cells [133], suggesting their potential use as
656 pan-monocyte markers. Interestingly, clone DH59B recognizes a conserved epitope across a wide
657 range of other species including small ruminants [134], dog [135], water buffalo [136] and dolphins
658 [137].
659 Although CD163 is a monocyte/macrophage differentiation antigen [138], and its expression in ncM
660 is very low or absent [16,17], it is still regarded as an important functional marker.
661 A multicolour panel designed for a proper resolution of these subsets should, therefore, contain the
662 markers: CD14, CD16, CD163, CD172a and a fluorescent dye for dead cell exclusion. Besides,
663 CD335 (NKp46) should also be used to exclude NK cells. In Table 5 a list of monoclonal antibodies
664 that can be used with either direct or indirect labelling protocols using anti-mouse secondary
665 fluorescent antibodies is reported, although labelling of monocytes is still a hot topic within the flow
666 cytometric community [55].
667 **Table 5.**
668 List of monoclonal antibodies reactive with bovine antigens
669

Specificity	Clone	Isotype	Target specie	Reference
CD14	CAM36A	IgG1	Bovine	[139]
	CAM66A	IgM	Caprine	[108]
	CC-G33	IgG1	Bovine	[140]
	M5E2	IgG2a	Human	[141]
	MM61A	IgG1	Bovine	[142]
	TÜK4	IgG2a	Human	[143]
	VPM65	IgG1	Ovine	[144]
CD16	KD1	IgG2a	Human	[145]
CD163	2A10/11	IgG1	Pig	[17]
	EDHu-1	IgG1	Human	[16]
	LND5A	IgG1	Bovine	[146]
	LND37A	IgG1	Bovine	[146]
	LND37A	IgG1	Bovine	[146]
CD172a	CC149	IgG2b	Bovine	[147]
	DH59B	IgG1	Bovine	[148]

670
671
672 A typical stain/lyse/wash protocol is the following:

1) 100 µL of whole blood anticoagulated with Heparin [149] are labelled with saturating concentrations of monoclonal antibodies (Table 5) in a final volume of 120 µL with PBS (pH 7.2), in a 5 mL polypropylene flow cytometric tube for 30 min at 4°C in the dark.
2) Erythrocytes are lysed with 1.0 mL of Tris-buffered ammonium chloride solution (0.87% w/v, pH 7.3) for 10 min, then 2 mL of cold PBS are added
3) The sample is centrifuged at 300 g for 5 min.
4) Pellet of labelled cells is re-suspended with 200 µL of cold PBS and immediately acquired by flow cytometry.

A simple indirect labelling protocol is done by introducing simple changes to the protocol previously described. In brief, whole blood is incubated under the same conditions with 0.75 µg of purified mAbs and then is processed in according to step 2 a 3. Pellet is re-suspended in 100 µL of fluorescent goat anti-mouse isotype-specific secondary mAbs and incubated for 15 min at 4°C in the dark. After the final wash, cells are re-suspended and acquired.

Appropriate controls are necessary to evaluate auto-fluorescence, background staining and proper sample compensation, as well as to perform a careful antibody titration.

The gating strategy to be used to identify the three subsets of monocytes should include: 1) time parameter *vs* FL or SSC to exclude event burst, 2) FSC-A *vs* FSC-H to exclude doublets, 3) exclusion of dead cells in the fluorescent live/dead channel, 4) FSC *vs* SSC to exclude debris and granulocytes from single live leukocytes, 5) CD172a *vs* CD16 dot plots to select CD172a positive mononuclear cells (all monocytes), 6) CD16 *vs* CD14 to separate cM subsets from intM and ncM, 7) back gating on dot plots 2, 3, and 4 to confirm the validity of the gating strategy.

To avoid false positives, the use of the fluorescence minus one (FMO) control for quadrant positions of the dot plot CD16 *vs* CD14 is recommended.

Pomeroy and coworkers [131] found a significant association between postpartum diseases (mastitis and metritis) and counts of monocyte subsets. Therefore, it is meaningful to evaluate the enumeration of absolute count of these subsets. Two different approaches can be used: dual-platform (flow cytometry and haematology) or single platform (flow cytometry). In the first method, the percentage of subsets (e.g. cM, intM, ncM) is measured with a flow cytometer while the absolute monocyte count is assessed by automated haematology analyzer. The absolute subset counts are therefore indirect. In the single-platform method, the flow cytometer is therefore used for directly counting monocyte subset in a given sample volume.

In humans, the precise and accurate leukocyte subset count (e.g. $CD4^+$ T cells in HIV patients, $CD34^+$ for autotransplantation) is of primary importance, and the two methods have been extensively described [150]. According to European Working Group on Clinical Cell Analysis (EWGCCA)

[135], the single-platform method should be regarded as the gold standard for absolute cell assessments, and the use of stain/lyse/no-wash labelling protocols is recommended.

9. Characterization of tissue macrophages via immunohistochemistry.

Circulating monocytes migrate into various tissues and transform into macrophages. Macrophages have several roles in tissues monitoring, inflammation and repair representing one of the dominant cell types in chronic inflammatory reactions.

Under non-inflammatory conditions, circulating monocytes localize in tissues and organs becoming resident macrophages to monitor healthy tissues. However, many resident macrophages are established before birth and then self- maintained during adult life. Resident macrophages are found in connective and adipose tissues, liver (Kupffer cells), splenic red pulp, bone marrow, lymph nodes, lung, brain, serous fluids, skin [151].

Under inflammatory conditions, most of the macrophages that accumulate at diseased sites typically derive from circulating monocytes and take on several functions according to the inciting factors and milieu including antigen presentation, phagocytosis, and immunomodulation through the production of various cytokines and growth factors. Macrophages can be classified based on their function and activation pathways. According to this grouping, there are classically-activated (M1) macrophages, wound-healing macrophages (also known as alternatively-activated (M2) macrophages), and regulatory macrophages (Mregs) [23,152,153].

Macrophages can be activated directly by bacterial lipopolysaccharides, via TLR and extracellular matrix proteins. Under T_H1 influence, macrophages react to IFN-γ, and TNF-α to become classically activated M1 macrophages producing Nitric Oxide and Reactive Oxygen Species and upregulating lysosomal enzymes to kill ingested organisms or digest foreign substances [23,152]. In T_H2 conditions macrophages act in response to IL-4, IL-5 and IL-13 by becoming wound healing M2 macrophages that secrete growth factors promoting angiogenesis, activating fibroblasts, and collagen synthesis [23,152]; under T regulatory secretion of IL-10 become regulatory/anti-inflammatory Mreg macrophages producing IL-10 to suppress inflammation [153].

9.1 Morphological characterization of macrophages: cytology and histology

Following tissue entry and activation, monocytes in tissue undergo functional and morphological transformation into reactive macrophages that are morphologically readily recognizable.

Thus, macrophages can be identified morphologically on cytological and histological specimens.

Cytological specimens are obtained by several techniques including imprints from tissues, scrapings to sample firm lesions which are less likely to exfoliate cells, swabs or by the needle aspiration technique. Sampled material by any of the aforementioned sampling methods can be smeared and air-dried [154]. Fluid specimens such as bronchoalveolar lavages, cerebrospinal fluid, articular fluid can be collected into an EDTA or a plain (if bacteriology is required) tube. Fluids can be cytocentrifuged or directly smeared according to their cellularity and again air-dried. Routine cytological stains are represented by alcohol-based Romanowsky type stains including May-Grünwald-Giemsa and Wright's stains [155].

On cytological specimens, macrophages are easy to identify:

a-Reactive macrophages (Fig. 6A) are cells characterized by round to irregular shape, variably large size (averaging18-30 μm), low N/C ratio, abundant light blue foamy to highly vacuolated cytoplasm with a paracentral to eccentric round to oval/reniform nucleus with granular chromatin and often one visible nucleolus. Macrophages phagocytize and degrade foreign exogenous or endogenous material and several etiological agents such as mycobacteria thus, they are recognized also because of their cytoplasmic content (Fig. 6B).

b-Multinucleated macrophagic giant cells are cells developing in persistent granulomatous inflammation by fusion of two or more activated macrophages in the attempt to engulf and degrade large or undigestible material or organisms. Multinucleated giant macrophages can be extremely large (40-80 μm), have two to multiple nuclei that may be haphazardly arranged termed foreign body type giant cells or have nuclei arranged at the periphery along the cell membrane in the so-called horseshoe fashion. These cells are named Langhans cells and develop commonly but are not exclusive of tuberculosis in humans as in cows.

c-Epithelioid macrophages develop in response to persistent intracellular pathogens such as mycobacteria. Epithelioid macrophages are characterized by large size, round to polygonal to spindle shape, abundant homogeneous light blue homogeneous, smooth cytoplasm with little to no vacuoles, an oval variably eccentric nucleus with finely granular chromatin. These cells are specialized in the production of cytokines and chemokines and do not have or have minimal phagocytic functions.

In tissue specimens, macrophages, their architectural organization and possibly the engulfed causative agent can be viewed by histology. For histological evaluation, tissues are fixed in 10% neutral phosphate-buffered formalin. Fixation in formalin provides a standardized method to immortalize tissues providing with optimal tissue architecture and morphology. Formalin is a solution of Formaldehyde fixing by adducts crosslink (methylene bridges) firming the tissue. Fixation times vary according to with type and size of tissues with a penetrance of 1mm per hour of

774 a 1 mm^3 tissue specimen with a volume of 1:10-1:20 with general fixation times of 24-48 h.
775 Following adequate fixations, tissues are routinely processed, dehydrated in graded alcohol scales to
776 remove free water, followed by tissue clearing (alcohol removal) in xylene and embedding in
777 paraffin. Tissue sections of 3-6 μm are cut, punt onto glass slides, dried, deparaffinized and stained
778 routinely with hematoxylin and eosin. Macrophage morphology is similar to that described for
779 cytological specimens (see the previous section) with observation or foamy reactive macrophages
780 with pink to grey granular to vacuolated cytoplasm with variably distinct cell boundaries (Fig. 6C),
781 multinucleated giant cells (Fig.6C and Fig. 6D) and epithelioid cells. Histopathology provides with
782 reduced cellular detail compared with cytology, however, give relevant information regarding the
783 organization of the inflammation. Specifically, granulomatous inflammation is a chronic
784 inflammation in which monocyte-macrophages predominate. Granulomatous inflammation can be
785 diffuse (lepromatous) with macrophages randomly dispersed in sheets (Fig. 6E) or nodular
786 (tuberculoid) with macrophages arranged in distinct masses termed granulomas (Fig. 6F). Diffuse
787 granulomatous inflammation is currently believed to derive from T_H2 driven stimuli while nodular
788 granulomatous inflammation derives from the predominance of T_H1 immunologic responses [156–
789 159]. The prototypic diffuse granulomatous inflammation in bovines is seen in Johne' diseases
790 where lamina propria of the intestine is expanded by sheets of macrophages (Fig. 6G associating to
791 a heavy cytoplasmic burden of *M. avium subsp. paratuberculosis* (Fig. 6H) and often with minimal
792 lymphoplasmacytic associated inflammation. In contrast, well-formed granulomas have a specific
793 stratigraphy. The prototype of nodular tuberculoid granuloma develops in bovines and humans
794 following *M. bovis* and *M. tuberculosis* infection. Granulomas in these conditions are generally
795 paucibacillary. Histologically, granulomas are recognized as caseating that is with a central core of
796 necrosis or non-caseating. Non-caseating granulomas contain a core of macrophages with variable
797 epithelioid and multinucleated giant cells and may be surrounded by mature lymphocytes, plasma
798 cells and rimmed by fibroblasts and collagen. Caseating granulomas have a similar arrangement but
799 with variably extensive central areas of necrosis and can be seen in bovine (Fig. 6I) and human
800 tuberculosis. In granulomas developing in the context of inflammatory reactions to persistent and
801 poorly degradable antigens (e.g. *Nocardia* spp., *Actinobacillus spp., Actinomyces spp., S. aureus*)
802 central accumulation of organisms rimmed and/or embedded in intensely eosinophilic material can
803 be seen. This material represents the accumulation of immunoglobulins and is termed splendore-
804 Hoeppli phenomenon (Fig. 6J). Furthermore, granulomas can be also formed after vaccine or alum
805 administration as described in many animal species including cats, dogs, swine, cattle and sheep.
806 Histochemical stains for macrophage identification are occasionally applied and include lysozyme
807 and acid phosphatase 5 [160] that however, should not be considered specific for macrophages.

9.2 Immunohistochemistry and Immunofluorescent characterization of macrophages.

Immunohistochemistry and immunofluorescence are techniques that have been utilized to identify macrophages and macrophage subpopulations by definition of their antigen surface expression. The phenotype of macrophages has been evaluated on cytological specimens, [161] frozen tissues and formalin-fixed, paraffin-embedded tissue specimens. Immunofluorescence is a technique that provides the same information of immunohistochemistry (protein expression by a cell or a tissue) but by activation of fluorescent dyes. Compared to immunohistochemistry, immunofluorescence allows for single and double stains on tissues with an easier interpretation of co-expression of antigens. However, immunofluorescence stained tissues need to be kept in the dark and must be evaluated with a fluorescence microscope. Tissue sections stained with fluorescent dyes need to be analysed promptly since fluorescence intensity decays rapidly (few days to few weeks). Also, autofluorescence interferes with the detection of specific fluorescent signals, especially when the signals of interest are very dim. Immunofluorescence is generally applied to frozen tissue sections while is seldom applied to formalin-fixed and paraffin-embedded samples because of tissue processing associates with increased autofluorescence that may interfere with positive immunofluorescent signals especially if these are dim. Additionally, immunofluorescent expression of markers on tissue macrophages should be interpreted with care since degradation components such as lipofuscins accumulating in macrophage cytoplasm are autofluorescent.
Immunohistochemistry is the most frequently applied technique to assess bovine macrophage phenotype in formalin-fixed tissue specimens, however, while formalin is the most common substance used worldwide for tissue fixation, induces cross-links (methylene bridges) that can block antibody access to antigenic epitopes or can damage surface antigens. To overcome antigen damage or masking caused by formalin fixation, immunofluorescence and immunohistochemistry can be applied to air-dried cytological specimens [162] or frozen tissue sections. Once the specimen is adequately sectioned immunohistochemistry and immunofluorescence techniques are similar. Immunohistochemistry on tissue sections has the advantage of visualizing protein expression in the context of the tissue, tissue lesion and specific cell type. This is less so for frozen specimens that bear inferior morphology and more so for immunofluorescence that reduces visualization of morphology. However, immunofluorescence is still favoured in specific studies because allows with easier double or multiple stains on tissues.
For immunohistochemistry, 3-6-μm sections are cut and put onto glued or charged slides to avoid detachment. Sections are deparaffinized and rehydrated using xylene and graded ethanol series. For

formalin-fixed tissue specimens in specific cases, antigen retrieval may be necessary. Antigen retrieval methods using enzymatic or heat-based protocols vary according to each molecular target and comprise: heat-induced (heating by pressure cookers or microwave in citrate buffer for 10 to 20 min), enzymatic (0.1% trypsin or pepsin in phosphate-buffered saline for 30 min at 37°C) or proteinase K (10 μg/mL proteinase K in Tris buffer for 15 min) may be necessary [163–168]. Endogenous peroxidase is quenched with 3% H_2O_2 in PBS or 3% H_2O_2 in methanol for 20-30 minutes to avoid false-positive results. Following washes in buffers, nonspecific antibody binding is inhibited by incubating tissues with blocking agents that vary according to primary and secondary antibody types and techniques. Primary antibody incubation temperatures (4-37°C) and times (1 hour to overnight) vary according to the reagents and techniques with longer incubation times favoured for paraffin-embedded tissue sections [164]. Secondary biotinylated antibody incubation and signal amplification with different systems such as avidin-biotin (ABC), streptavidin-peroxidase complexes are followed by visualization with chromogens such as 3, 3′-diaminobenzidine or 3-Amino-9-ethyl carbazole (AEC) carbazole and counterstained with hematoxylin.

For immunofluorescence, tissue specimens should be snap-frozen in isopentane cooled at the freezing temperature by immersion in liquid nitrogen. Frozen samples should be stored at -80˚C or cut on a cryostat immediately after freezing. For immunofluorescence, sections are dried and autofluorescence is quenched with 3-3 DAB. The following steps parallel those described for immunohistochemistry. Primary antibodies can be directly labelled with the fluorescent dyes thus the secondary antibodies and steps involving amplification of the signal and visualization with chromogens can be avoided. If primary antibodies are unconjugated, visualization is achieved by incubating the samples with the specific secondary antibody generally conjugated to rhodamine or FITC. Nuclei can be counterstained with 4’,6- diamidino-2-phenylindole, dihydrochloride (DAPI) or Hoechst 33342.

Dual-colour immunofluorescence has been seldom applied to bovine tissues for macrophage evaluation [169].

Table. 5
List and details of molecular targets utilized for the immunohistochemical or immunofluorescent examination of bovine macrophages in formalin-fixed or frozen tissue sections.

Primary Ab Target	Main cellular expression	Known or proposed functions	IHC/IF	Ref.
CD14	Monocytes, Macrophages	Coreceptor for bacterial LPS, recruiting LPS to TLR, clearance of apoptotic cells,	IF	[169,170]
CD11b	Monocytes, Macrophages, natural killer cells, neutrophil granulocytes,	Heterodimer binding to beta integrin CD18 (Mac-1 complex) mediating leukocyte adhesion and migration	IF	[169]
CD68	Monocytes, Macrophages, Osteoclasts	Lysosomal membrane activated phagocytosis	IHC, IF	[138, 141–143]
CD107b	Placenta, lung and liver (wide tissue distribution), activated neutrophil granulocytes, activated platelets, activated T cells, activated endothelium	Modulates chaperone-mediated autophagy. Decreases presentation of endogenous antigens by MHCII Maintenance of lysosomal integrity, pH and catabolism	IF	[160]
CD163	Monocytes, Macrophages, M2 polarization	Acute phase-regulated receptor, clearance and endocytosis of haemoglobin/haptoglobin complexes by macrophages (protect tissues from free haemoglobin-mediated oxidative damage). Innate immune sensor for bacteria inducer of proinflammatory cytokine production	IF, IHC	[136–138,144–147]
CD172a	Neutrophil granulocytes, Monocytes, Macrophages M2 polarization	Receptor-type transmembrane glycoprotein negative regulator of receptor tyrosine kinase-coupled signalling	IHC	[175,176]
CD204	Myeloid cells	Endocytosis of modified/oxidized low-density lipoproteins	IHC	[163]
CD206	Macrophages, Immature Dendritic cells	Scavenger receptor that binding and internalization and lysosomal transport of microbial high mannose oligosaccharides	IF	[173]
Iba-1	Activated macrophages,	Actin and calcium-binding protein with a role in Chemotaxis. Induced by cytokines and interferon promote	IHC	[163,166,167,171]

	Microglia, activated endothelial cells Neutrophils	macrophage activation and growth of vascular smooth muscle cells and T-lymphocytes.		
Mac387	Granulocytes, Monocytes, Macrophages	calcium- and zinc-binding protein with proinflammatory, antimicrobial, oxidant-scavenging and apoptosis-inducing activities.	IHC	[166]
Nramp-1	Monocytes, Macrophages	Role in resistance to intracellular bacterial pathogens	IHC	[165]

CD14 (Monocyte Differentiation Antigen CD14), CD11b (Integrin alpha), CD68 (Scavenger Receptor Class D, LAMP4, SCARD1), CD107b (Mac3, LAMP2-lysosomal associated membrane protein 2), CD163 (AM-3K, Scavenger Receptor Cysteine-Rich Type 1 Protein M130), CD172a (SIRPA, Signal Regulatory Protein Alpha), CD204 (MSR1, Macrophage scavenger receptor 1), CD206 (Mannose receptor MRC1), Iba-1 (Ionizing binding adaptor molecule 1, Allograft inflammatory factor 1 - AIF-1), Mac387 (Calprotectin beta chain), Nramp-1 (Natural resistance-associated macrophage protein 1)

Table 6. List of molecular targets used for the immunohistochemical or immunofluorescent identification of bovine macrophage M1/M2 polarization in formalin-fixed or frozen tissue sections.

Cytokine target	M1/M2 Polarization	Technique	Disease	Ref.
IFNγ	M1	IF, IHC	Paratuberculosis	[166,173]
IL1Ra	M2	IF	Paratuberculosis	[173]
IL1-β	M1	IF, IHC	Paratuberculosis Contagious pleuropneumonia	[173,177]
IL-10	Mreg	IF	Paratuberculosis	[165,173]
IL-12p40	M1	IF	Paratuberculosis	[173]
IL-17A	M1	IHC	Contagious pleuropneumonia	[177]
IL-23	M1	IF	Paratuberculosis	[173]
iNOS	M1	IHC	Paratuberculosis	[165]
TGF-β	M2	IF, IHC	Paratuberculosis	[165,173]
TLR4 (CD284)	M1	IF	Paratuberculosis	[173]
TNF-α	M1	IF, IHC	Paratuberculosis Contagious pleuropneumonia	[165,173,177]
uNOS (all NOS isoforms)	M1	IF	Paratuberculosis	[173]

Several molecular targets have been utilized for the identification of bovine macrophages in formalin-fixed (Fig. 6K) or frozen tissue specimens. The molecular targets for macrophage recognition in cattle, their function and corresponding references are listed in Table 5. Immunohistochemistry and immunofluorescence have been utilized to identify, enumerate and characterize tissue macrophages in formalin-fixed [160,163–167,175–177] or frozen [168–170,172–174] sections of a variety of bovine tissue samples including adipose tissue [160,167,168,175], in the intestinal tissue of cattle with spontaneous paratuberculosis at different stages of the disease [165,166,172–174], the endometrium of pregnant and post parturient dairy cows [169,170,176], fibrotic liver lesions in bovines infected with *Fasciola hepatica* [163], lung lesion in bovine contagious pleuropneumonia [177] and early lesions during experimental *M. bovis* aerosol infection [164].

Polarization of M1-host defence macrophages versus M2-resolution/tissue repair macrophages has been investigated on tissue sections in bovine paratuberculosis and contagious bovine pleuropneumonia [165,173,177]. The target molecules assessed to study bovine macrophage polarization in tissues comprise several cytokines (Fig. 6L) and are listed in Table 6. Regarding macrophage polarization, the evaluation of CD163 expression as a specific marker form M2 polarization has been questioned [174] because of its widespread expression in macrophages independently of disease stage of bovine paratuberculosis. Thus, CD163 is now favoured as a marker for all bovine macrophages and this reason has been listed in Table 5 and not in Table 6. Studies on paratuberculosis have demonstrated significantly higher numbers of M2 macrophages in the ileum of bovines with the clinical stage multibacillary lesions [165,173]. On the contrary, significant polarization versus M1 phenotype has been observed in paucibacillary lesions [166]. In lung lesions of contagious bovine pleuropneumonia, a general M1 polarization has been detected [177].

10. Conclusions

The present work reviews the current methods to classify in subpopulations and study the main functions of monocyte and macrophages in bovine species. The concept of monocyte/macrophage polarization in subsets has been validated and accepted in bovine species, and monocyte distribution in blood, and macrophage in tissues, mostly resembles that of human species. Indeed, new knowledge on monocyte and macrophage function basic biology and functions is needed to understand their impact on immune response in cows. Further studies are needed to demonstrate if monocytes can be further classified in subsets and to determine what is the function of each sub-set in bovine species as well. Among the various techniques applied so far, flow cytometry is the most promising and rapid method to identify new monocyte populations in bovine species and study their functions. The

application of flow cytometry in veterinary medicine has lagged behind human medical uses: the number of specific antibodies is limited, and the cross-reactivity of most of those available for human and murine studies is not validated in cows. The lack of specific reagents is what holds major challenges in advancing the knowledge in bovine monocytes. Lacking a labelled anti-Cd16 antibody allowing purification of ncM and intM is what prevents a full understanding of the functions of these important sub-classes of monocytes in the cow. Transcriptome analysis of resting and activated monocytes and macrophages is also limited to few studies: the role of different monocyte subset would be much more clear with a system biology approach by integrating transcriptome, metabolome, proteome and microRNAome of each subset after inflammatory activation.

This information would provide important advancement in diagnosis and investigation of the pathogenesis of important cattle diseases, such for example tuberculosis, brucellosis or Johne's disease that affect human health as well.

References

[1] G. Lauvau, L. Chorro, E. Spaulding, S.M. Soudja, Inflammatory monocyte effector mechanisms., Cell. Immunol. 291 (n.d.) 32–40. https://doi.org/10.1016/j.cellimm.2014.07.007.

[2] P.J. Murray, T.A. Wynn, Protective and pathogenic functions of macrophage subsets., Nat. Rev. Immunol. 11 (2011) 723–37. https://doi.org/10.1038/nri3073.

[3] C.G. Chitko-McKown, F. Blecha, Pulmonary intravascular macrophages: a review of immune properties and functions., Ann. Rech. Vet. 23 (1992) 201–14. http://www.ncbi.nlm.nih.gov/pubmed/1416724.

[4] S. Arora, K. Dev, B. Agarwal, P. Das, M.A. Syed, Macrophages: Their role, activation and polarization in pulmonary diseases., Immunobiology. 223 (n.d.) 383–396. https://doi.org/10.1016/j.imbio.2017.11.001.

[5] J. Herz, A.J. Filiano, A. Smith, N. Yogev, J. Kipnis, Myeloid Cells in the Central Nervous System, Immunity. 46 (2017) 943–956. https://doi.org/10.1016/j.immuni.2017.06.007.

[6] A. Fani Maleki, S. Rivest, Innate Immune Cells: Monocytes, Monocyte-Derived Macrophages and Microglia as Therapeutic Targets for Alzheimer's Disease and Multiple Sclerosis., Front. Cell. Neurosci. 13 (2019) 355. https://doi.org/10.3389/fncel.2019.00355.

[7] P. Thériault, A. ElAli, S. Rivest, The dynamics of monocytes and microglia in Alzheimer's disease., Alzheimers. Res. Ther. 7 (2015) 41. https://doi.org/10.1186/s13195-015-0125-2.

[8] T.A. Wynn, A. Chawla, J.W. Pollard, Macrophage biology in development, homeostasis and disease.,

Nature. 496 (2013) 445–55. https://doi.org/10.1038/nature12034.

[9] T. Joeris, K. Müller-Luda, W.W. Agace, A.M. Mowat, Diversity and functions of intestinal mononuclear phagocytes., Mucosal Immunol. 10 (2017) 845–864. https://doi.org/10.1038/mi.2017.22.

[10] S. Wang, Q. Ye, X. Zeng, S. Qiao, Functions of Macrophages in the Maintenance of Intestinal Homeostasis., J. Immunol. Res. 2019 (2019) 1512969. https://doi.org/10.1155/2019/1512969.

[11] T. Ganz, Macrophages and systemic iron homeostasis., J. Innate Immun. 4 (2012) 446–53. https://doi.org/10.1159/000336423.

[12] B.S. Steiniger, Human spleen microanatomy: why mice do not suffice., Immunology. 145 (2015) 334–46. https://doi.org/10.1111/imm.12469.

[13] C. Zannetti, G. Roblot, E. Charrier, M. Ainouze, I. Tout, F. Briat, N. Isorce, S. Faure-Dupuy, M. Michelet, M. Marotel, S. Kati, T.F. Schulz, M. Rivoire, A. Traverse-Glehen, S. Luangsay, O. Alatiff, T. Henry, T. Walzer, D. Durantel, U. Hasan, Characterization of the Inflammasome in Human Kupffer Cells in Response to Synthetic Agonists and Pathogens., J. Immunol. 197 (2016) 356–67. https://doi.org/10.4049/jimmunol.1502301.

[14] B. Passlick, D. Flieger, H.W. Ziegler-Heitbrock, Identification and characterization of a novel monocyte subpopulation in human peripheral blood., Blood. 74 (1989) 2527–34. http://www.ncbi.nlm.nih.gov/pubmed/2478233.

[15] P. Ancuta, R. Rao, A. Moses, A. Mehle, S.K. Shaw, F.W. Luscinskas, D. Gabuzda, Fractalkine Preferentially Mediates Arrest and Migration of CD16+ Monocytes, J. Exp. Med. 197 (2003) 1701–1707. https://doi.org/10.1084/jem.20022156.

[16] L. Ziegler-Heitbrock, P. Ancuta, S. Crowe, M. Dalod, V. Grau, D.N. Hart, P.J.M. Leenen, Y.-J. Liu, G. MacPherson, G.J. Randolph, J. Scherberich, J. Schmitz, K. Shortman, S. Sozzani, H. Strobl, M. Zembala, J.M. Austyn, M.B. Lutz, Nomenclature of monocytes and dendritic cells in blood, Blood. 116 (2010) e74–e80. https://doi.org/10.1182/blood-2010-02-258558.

[17] Y. Corripio-Miyar, J. Hope, C.J. McInnes, S.R. Wattegedera, K. Jensen, Y. Pang, G. Entrican, E.J. Glass, Phenotypic and functional analysis of monocyte populations in cattle peripheral blood identifies a subset with high endocytic and allogeneic T-cell stimulatory capacity, Vet. Res. 46 (2015) 112. https://doi.org/10.1186/s13567-015-0246-4.

[18] J. Hussen, A. Düvel, O. Sandra, D. Smith, I.M. Sheldon, P. Zieger, H.-J. Schuberth, Phenotypic and Functional Heterogeneity of Bovine Blood Monocytes, PLoS One. 8 (2013) e71502. https://doi.org/10.1371/journal.pone.0071502.

[19] J. Hussen, H.-J. Schuberth, Heterogeneity of Bovine Peripheral Blood Monocytes., Front. Immunol. 8

(2017) 1875. https://doi.org/10.3389/fimmu.2017.01875.

[20] J. Hussen, A. Düvel, M. Koy, H.-J. Schuberth, Inflammasome activation in bovine monocytes by extracellular ATP does not require the purinergic receptor P2X7, Dev. Comp. Immunol. 38 (2012) 312–320. https://doi.org/10.1016/j.dci.2012.06.004.

[21] G. Zizzo, P.L. Cohen, IL-17 stimulates differentiation of human anti-inflammatory macrophages and phagocytosis of apoptotic neutrophils in response to IL-10 and glucocorticoids., J. Immunol. 190 (2013) 5237–46. https://doi.org/10.4049/jimmunol.1203017.

[22] J.R. de Sousa, P.F. Da Costa Vasconcelos, J.A.S. Quaresma, Functional aspects, phenotypic heterogeneity, and tissue immune response of macrophages in infectious diseases., Infect. Drug Resist. 12 (2019) 2589–2611. https://doi.org/10.2147/IDR.S208576.

[23] P.J. Murray, J.E. Allen, S.K. Biswas, E.A. Fisher, D.W. Gilroy, S. Goerdt, S. Gordon, J.A. Hamilton, L.B. Ivashkiv, T. Lawrence, M. Locati, A. Mantovani, F.O. Martinez, J.-L. Mege, D.M. Mosser, G. Natoli, J.P. Saeij, J.L. Schultze, K.A. Shirey, A. Sica, J. Suttles, I. Udalova, J.A. van Ginderachter, S.N. Vogel, T.A. Wynn, Macrophage activation and polarization: nomenclature and experimental guidelines., Immunity. 41 (2014) 14–20. https://doi.org/10.1016/j.immuni.2014.06.008.

[24] A. Mantovani, A. Sica, S. Sozzani, P. Allavena, A. Vecchi, M. Locati, The chemokine system in diverse forms of macrophage activation and polarization., Trends Immunol. 25 (2004) 677–86. https://doi.org/10.1016/j.it.2004.09.015.

[25] S. Colin, G. Chinetti-Gbaguidi, B. Staels, Macrophage phenotypes in atherosclerosis, Immunol. Rev. 262 (2014) 153–166. https://doi.org/10.1111/imr.12218.

[26] M.H. Abdelaziz, S.F. Abdelwahab, J. Wan, W. Cai, W. Huixuan, C. Jianjun, K.D. Kumar, A. Vasudevan, A. Sadek, Z. Su, S. Wang, H. Xu, Alternatively activated macrophages; a double-edged sword in allergic asthma., J. Transl. Med. 18 (2020) 58. https://doi.org/10.1186/s12967-020-02251-w.

[27] L. Wang, S. Zhang, H. Wu, X. Rong, J. Guo, M2b macrophage polarization and its roles in diseases, J. Leukoc. Biol. 106 (2019) 345–358. https://doi.org/10.1002/JLB.3RU1018-378RR.

[28] A. Shapouri-Moghaddam, S. Mohammadian, H. Vazini, M. Taghadosi, S.-A. Esmaeili, F. Mardani, B. Seifi, A. Mohammadi, J.T. Afshari, A. Sahebkar, Macrophage plasticity, polarization, and function in health and disease., J. Cell. Physiol. 233 (2018) 6425–6440. https://doi.org/10.1002/jcp.26429.

[29] I. Malyshev, Y. Malyshev, Current Concept and Update of the Macrophage Plasticity Concept: Intracellular Mechanisms of Reprogramming and M3 Macrophage “Switch” Phenotype, Biomed Res. Int. 2015 (2015) 1–22. https://doi.org/10.1155/2015/341308.

[30] C. Jackaman, T.L. Yeoh, M.L. Acuil, J.K. Gardner, D.J. Nelson, Murine mesothelioma induces locally-proliferating IL-10(+)TNF-α(+)CD206(-)CX3CR1(+) M3 macrophages that can be selectively

depleted by chemotherapy or immunotherapy., Oncoimmunology. 5 (2016) e1173299. https://doi.org/10.1080/2162402X.2016.1173299.

[31] H. Jinnouchi, L. Guo, A. Sakamoto, S. Torii, Y. Sato, A. Cornelissen, S. Kuntz, K.H. Paek, R. Fernandez, D. Fuller, N. Gadhoke, D. Surve, M. Romero, F.D. Kolodgie, R. Virmani, A. V Finn, Diversity of macrophage phenotypes and responses in atherosclerosis., Cell. Mol. Life Sci. (2019). https://doi.org/10.1007/s00018-019-03371-3.

[32] M. de la Paz Sánchez-Martínez, F. Blanco-Favela, M.D. Mora-Ruiz, A.K. Chávez-Rueda, M. Bernabe-García, L. Chávez-Sánchez, IL-17-differentiated macrophages secrete pro-inflammatory cytokines in response to oxidized low-density lipoprotein., Lipids Health Dis. 16 (2017) 196. https://doi.org/10.1186/s12944-017-0588-1.

[33] P. Riquelme, J. Haarer, A. Kammler, L. Walter, S. Tomiuk, N. Ahrens, A.K. Wege, I. Goecze, D. Zecher, B. Banas, R. Spang, F. Fändrich, M.B. Lutz, B. Sawitzki, H.J. Schlitt, J. Ochando, E.K. Geissler, J.A. Hutchinson, TIGIT+ iTregs elicited by human regulatory macrophages control T cell immunity., Nat. Commun. 9 (2018) 2858. https://doi.org/10.1038/s41467-018-05167-8.

[34] A. Kadl, A.K. Meher, P.R. Sharma, M.Y. Lee, A.C. Doran, S.R. Johnstone, M.R. Elliott, F. Gruber, J. Han, W. Chen, T. Kensler, K.S. Ravichandran, B.E. Isakson, B.R. Wamhoff, N. Leitinger, Identification of a novel macrophage phenotype that develops in response to atherogenic phospholipids via Nrf2., Circ. Res. 107 (2010) 737–46. https://doi.org/10.1161/CIRCRESAHA.109.215715.

[35] D.A. Chistiakov, Y. V Bobryshev, A.N. Orekhov, Changes in transcriptome of macrophages in atherosclerosis., J. Cell. Mol. Med. 19 (2015) 1163–73. https://doi.org/10.1111/jcmm.12591.

[36] S.C. Talker, A. Baumann, G.T. Barut, I. Keller, R. Bruggmann, A. Summerfield, Precise Delineation and Transcriptional Characterization of Bovine Blood Dendritic-Cell and Monocyte Subsets., Front. Immunol. 9 (2018) 2505. https://doi.org/10.3389/fimmu.2018.02505.

[37] K.L. Wong, J.J.-Y. Tai, W.-C. Wong, H. Han, X. Sem, W.-H. Yeap, P. Kourilsky, S.-C. Wong, Gene expression profiling reveals the defining features of the classical, intermediate, and nonclassical human monocyte subsets, Blood. 118 (2011) e16–e31. https://doi.org/10.1182/blood-2010-12-326355.

[38] P. Italiani, D. Boraschi, From Monocytes to M1/M2 Macrophages: Phenotypical vs. Functional Differentiation, Front. Immunol. 5 (2014). https://doi.org/10.3389/fimmu.2014.00514.

[39] L. Ziegler-Heitbrock, T.P.J. Hofer, Toward a Refined Definition of Monocyte Subsets, Front. Immunol. 4 (2013). https://doi.org/10.3389/fimmu.2013.00023.

[40] A. MANTOVANI, S. SOZZANI, M. LOCATI, P. ALLAVENA, A. SICA, Macrophage polarization:

tumor-associated macrophages as a paradigm for polarized M2 mononuclear phagocytes, Trends Immunol. 23 (2002) 549–555. https://doi.org/10.1016/S1471-4906(02)02302-5.

[41] J. Kramer, Normal Hematology of Cattle, Cheep, and Goats, in: B. Feldman, J. Zinkl, N. Jain (Eds.), Vet. Hematol., 5th ed., Lippincott Williams & Wilkins, Baltimore, 2000: pp. 1075–1084.

[42] B.M. Goddeeris, C.L. Baldwin, O. Ole-MoiYoi, W.I. Morrison, Improved methods for purification and depletion of monocytes from bovine peripheral blood mononuclear cells. Functional evaluation of monocytes in responses to lectins., J. Immunol. Methods. 89 (1986) 165–73. https://doi.org/10.1016/0022-1759(86)90354-6.

[43] F. Ceciliani, V. Pocacqua, A. Miranda-Ribera, V. Bronzo, C. Lecchi, P. Sartorelli, alpha(1)-Acid glycoprotein modulates apoptosis in bovine monocytes., Vet. Immunol. Immunopathol. 116 (2007) 145–152. https://doi.org/10.1016/j.vetimm.2007.01.006.

[44] C. Lecchi, A. Scarafoni, V. Bronzo, P.A. Martino, A. Cavallini, P. Sartorelli, F. Ceciliani, Alpha1-Acid glycoprotein modulates phagocytosis and killing of Escherichia coli by bovine polymorphonuclear leucocytes and monocytes, Vet. J. 196 (2013) 47–51. https://doi.org/10.1016/j.tvjl.2012.07.022.

[45] J. Vives, M. Parra, R. Castillo, Platelet aggregation technique used in the preparation of lymphocyte suspensions., Tissue Antigens. 1 (1971) 276–8. https://doi.org/10.1111/j.1399-0039.1971.tb00106.x.

[46] R.J. Perper, T.W. Zee, M.M. Mickelson, Purification of lymphocytes and platelets by gradient centrifugation., J. Lab. Clin. Med. 72 (1968) 842–8. http://www.ncbi.nlm.nih.gov/pubmed/5697393.

[47] T. Vanden Berghe, S. Grootjans, V. Goossens, Y. Dondelinger, D. V Krysko, N. Takahashi, P. Vandenabeele, Determination of apoptotic and necrotic cell death in vitro and in vivo, Methods. 61 (2013) 117–129. https://doi.org/https://doi.org/10.1016/j.ymeth.2013.02.011.

[48] L. Galluzzi, I. Vitale, S.A. Aaronson, J.M. Abrams, D. Adam, P. Agostinis, E.S. Alnemri, L. Altucci, I. Amelio, D.W. Andrews, M. Annicchiarico-Petruzzelli, A. V. Antonov, E. Arama, E.H. Baehrecke, N.A. Barlev, N.G. Bazan, F. Bernassola, M.J.M. Bertrand, K. Bianchi, M. V. Blagosklonny, K. Blomgren, C. Borner, P. Boya, C. Brenner, M. Campanella, E. Candi, D. Carmona-Gutierrez, F. Cecconi, F.K.-M. Chan, N.S. Chandel, E.H. Cheng, J.E. Chipuk, J.A. Cidlowski, A. Ciechanover, G.M. Cohen, M. Conrad, J.R. Cubillos-Ruiz, P.E. Czabotar, V. D'Angiolella, T.M. Dawson, V.L. Dawson, V. De Laurenzi, R. De Maria, K.-M. Debatin, R.J. DeBerardinis, M. Deshmukh, N. Di Daniele, F. Di Virgilio, V.M. Dixit, S.J. Dixon, C.S. Duckett, B.D. Dynlacht, W.S. El-Deiry, J.W. Elrod, G.M. Fimia, S. Fulda, A.J. García-Sáez, A.D. Garg, C. Garrido, E. Gavathiotis, P. Golstein, E. Gottlieb, D.R. Green, L.A. Greene, H. Gronemeyer, A. Gross, G. Hajnoczky, J.M. Hardwick, I.S. Harris, M.O. Hengartner, C. Hetz, H. Ichijo, M. Jäättelä, B. Joseph, P.J. Jost, P.P. Juin, W.J. Kaiser, M. Karin, T. Kaufmann, O. Kepp, A. Kimchi, R.N. Kitsis, D.J. Klionsky, R.A. Knight, S. Kumar,

S.W. Lee, J.J. Lemasters, B. Levine, A. Linkermann, S.A. Lipton, R.A. Lockshin, C. López-Otín, S.W. Lowe, T. Luedde, E. Lugli, M. MacFarlane, F. Madeo, M. Malewicz, W. Malorni, G. Manic, J.-C. Marine, S.J. Martin, J.-C. Martinou, J.P. Medema, P. Mehlen, P. Meier, S. Melino, E.A. Miao, J.D. Molkentin, U.M. Moll, C. Muñoz-Pinedo, S. Nagata, G. Nuñez, A. Oberst, M. Oren, M. Overholtzer, M. Pagano, T. Panaretakis, M. Pasparakis, J.M. Penninger, D.M. Pereira, S. Pervaiz, M.E. Peter, M. Piacentini, P. Pinton, J.H.M. Prehn, H. Puthalakath, G.A. Rabinovich, M. Rehm, R. Rizzuto, C.M.P. Rodrigues, D.C. Rubinsztein, T. Rudel, K.M. Ryan, E. Sayan, L. Scorrano, F. Shao, Y. Shi, J. Silke, H.-U. Simon, A. Sistigu, B.R. Stockwell, A. Strasser, G. Szabadkai, S.W.G. Tait, D. Tang, N. Tavernarakis, A. Thorburn, Y. Tsujimoto, B. Turk, T. Vanden Berghe, P. Vandenabeele, M.G. Vander Heiden, A. Villunger, H.W. Virgin, K.H. Vousden, D. Vucic, E.F. Wagner, H. Walczak, D. Wallach, Y. Wang, J.A. Wells, W. Wood, J. Yuan, Z. Zakeri, B. Zhivotovsky, L. Zitvogel, G. Melino, G. Kroemer, Molecular mechanisms of cell death: recommendations of the Nomenclature Committee on Cell Death 2018, Cell Death Differ. 25 (2018) 486–541. https://doi.org/10.1038/s41418-017-0012-4.

[49] G. Kroemer, W.S. El-Deiry, P. Golstein, M.E. Peter, D. Vaux, P. Vandenabeele, B. Zhivotovsky, M. V Blagosklonny, W. Malorni, R.A. Knight, M. Piacentini, S. Nagata, G. Melino, Classification of cell death: recommendations of the Nomenclature Committee on Cell Death, Cell Death Differ. 12 (2005) 1463–1467. https://doi.org/10.1038/sj.cdd.4401724.

[50] J.F. Kerr, A.H. Wyllie, A.R. Currie, Apoptosis: a basic biological phenomenon with wide-ranging implications in tissue kinetics, Br. J. Cancer. 26 (1972) 239–257. https://doi.org/10.1038/bjc.1972.33.

[51] G. Denecker, D. Vercammen, M. Steemans, T. Vanden Berghe, G. Brouckaert, G. Van Loo, B. Zhivotovsky, W. Fiers, J. Grooten, W. Declercq, P. Vandenabeele, Death receptor-induced apoptotic and necrotic cell death: differential role of caspases and mitochondria, Cell Death Differ. 8 (2001) 829—840. https://doi.org/10.1038/sj.cdd.4400883.

[52] G. van Loo, X. Saelens, M. van Gurp, M. MacFarlane, S.J. Martin, P. Vandenabeele, The role of mitochondrial factors in apoptosis: a Russian roulette with more than one bullet, Cell Death Differ. 9 (2002) 1031–1042. https://doi.org/10.1038/sj.cdd.4401088.

[53] S. Elmore, Apoptosis: a review of programmed cell death, Toxicol. Pathol. 35 (2007) 495–516. https://doi.org/10.1080/01926230701320337.

[54] M.S. D'Arcy, Cell death: a review of the major forms of apoptosis, necrosis and autophagy, Cell Biol. Int. 43 (2019) 582–592. https://doi.org/10.1002/cbin.11137.

[55] A. Cossarizza, H.-D. Chang, A. Radbruch, A. Acs, D. Adam, S. Adam-Klages, W.W. Agace, N. Aghaeepour, M. Akdis, M. Allez, L.N. Almeida, G. Alvisi, G. Anderson, I. Andrä, F. Annunziato, A. Anselmo, P. Bacher, C.T. Baldari, S. Bari, V. Barnaba, J. Barros-Martins, L. Battistini, W. Bauer, S. Baumgart, N. Baumgarth, D. Baumjohann, B. Baying, M. Bebawy, B. Becher, W. Beisker, V. Benes,

R. Beyaert, A. Blanco, D.A. Boardman, C. Bogdan, J.G. Borger, G. Borsellino, P.E. Boulais, J.A. Bradford, D. Brenner, R.R. Brinkman, A.E.S. Brooks, D.H. Busch, M. Büscher, T.P. Bushnell, F. Calzetti, G. Cameron, I. Cammarata, X. Cao, S.L. Cardell, S. Casola, M.A. Cassatella, A. Cavani, A. Celada, L. Chatenoud, P.K. Chattopadhyay, S. Chow, E. Christakou, L. Čičin-Šain, M. Clerici, F.S. Colombo, L. Cook, A. Cooke, A.M. Cooper, A.J. Corbett, A. Cosma, L. Cosmi, P.G. Coulie, A. Cumano, L. Cvetkovic, V.D. Dang, C. Dang-Heine, M.S. Davey, D. Davies, S. De Biasi, G. Del Zotto, G.V. Dela Cruz, M. Delacher, S. Della Bella, P. Dellabona, G. Deniz, M. Dessing, J.P. Di Santo, A. Diefenbach, F. Dieli, A. Dolf, T. Dörner, R.J. Dress, D. Dudziak, M. Dustin, C.-A. Dutertre, F. Ebner, S.B.G. Eckle, M. Edinger, P. Eede, G.R.A. Ehrhardt, M. Eich, P. Engel, B. Engelhardt, A. Erdei, C. Esser, B. Everts, M. Evrard, C.S. Falk, T.A. Fehniger, M. Felipo-Benavent, H. Ferry, M. Feuerer, A. Filby, K. Filkor, S. Fillatreau, M. Follo, I. Förster, J. Foster, G.A. Foulds, B. Frehse, P.S. Frenette, S. Frischbutter, W. Fritzsche, D.W. Galbraith, A. Gangaev, N. Garbi, B. Gaudilliere, R.T. Gazzinelli, J. Geginat, W. Gerner, N.A. Gherardin, K. Ghoreschi, L. Gibellini, F. Ginhoux, K. Goda, D.I. Godfrey, C. Goettlinger, J.M. González-Navajas, C.S. Goodyear, A. Gori, J.L. Grogan, D. Grummitt, A. Grützkau, C. Haftmann, J. Hahn, H. Hammad, G. Hämmerling, L. Hansmann, G. Hansson, C.M. Harpur, S. Hartmann, A. Hauser, A.E. Hauser, D.L. Haviland, D. Hedley, D.C. Hernández, G. Herrera, M. Herrmann, C. Hess, T. Höfer, P. Hoffmann, K. Hogquist, T. Holland, T. Höllt, R. Holmdahl, P. Hombrink, J.P. Houston, B.F. Hoyer, B. Huang, F.-P. Huang, J.E. Huber, J. Huehn, M. Hundemer, C.A. Hunter, W.Y.K. Hwang, A. Iannone, F. Ingelfinger, S.M. Ivison, H.-M. Jäck, P.K. Jani, B. Jávega, S. Jonjic, T. Kaiser, T. Kalina, T. Kamradt, S.H.E. Kaufmann, B. Keller, S.L.C. Ketelaars, A. Khalilnezhad, S. Khan, J. Kisielow, P. Klenerman, J. Knopf, H.-F. Koay, K. Kobow, J.K. Kolls, W.T. Kong, M. Kopf, T. Korn, K. Kriegsmann, H. Kristyanto, T. Kroneis, A. Krueger, J. Kühne, C. Kukat, D. Kunkel, H. Kunze-Schumacher, T. Kurosaki, C. Kurts, P. Kvistborg, I. Kwok, J. Landry, O. Lantz, P. Lanuti, F. LaRosa, A. Lehuen, S. LeibundGut-Landmann, M.D. Leipold, L.Y.T. Leung, M.K. Levings, A.C. Lino, F. Liotta, V. Litwin, Y. Liu, H.-G. Ljunggren, M. Lohoff, G. Lombardi, L. Lopez, M. López-Botet, A.E. Lovett-Racke, E. Lubberts, H. Luche, B. Ludewig, E. Lugli, S. Lunemann, H.T. Maecker, L. Maggi, O. Maguire, F. Mair, K.H. Mair, A. Mantovani, R.A. Manz, A.J. Marshall, A. Martínez-Romero, G. Martrus, I. Marventano, W. Maslinski, G. Matarese, A.V. Mattioli, C. Maueröder, A. Mazzoni, J. McCluskey, M. McGrath, H.M. McGuire, I.B. McInnes, H.E. Mei, F. Melchers, S. Melzer, D. Mielenz, S.D. Miller, K.H.G. Mills, H. Minderman, J. Mjösberg, J. Moore, B. Moran, L. Moretta, T.R. Mosmann, S. Müller, G. Multhoff, L.E. Muñoz, C. Münz, T. Nakayama, M. Nasi, K. Neumann, L.G. Ng, A. Niedobitek, S. Nourshargh, G. Núñez, J.-E. O'Connor, A. Ochel, A. Oja, D. Ordonez, A. Orfao, E. Orlowski-Oliver, W. Ouyang, A. Oxenius, R. Palankar, I. Panse, K. Pattanapanyasat, M. Paulsen, D. Pavlinic, L. Penter, P. Peterson, C. Peth, J. Petriz, F. Piancone, W.F. Pickl, S. Piconese, M. Pinti, A.G. Pockley, M.J. Podolska, Z. Poon, K. Pracht, I. Prinz, C.E.M. Pucillo, S.A. Quataert, L. Quatrini, K.M. Quinn, H. Radbruch, T.R.D.J. Radstake, S. Rahmig, H.-P. Rahn, B. Rajwa, G. Ravichandran,

Y. Raz, J.A. Rebhahn, D. Recktenwald, D. Reimer, C. Reis E Sousa, E.B.M. Remmerswaal, L. Richter, L.G. Rico, A. Riddell, A.M. Rieger, J.P. Robinson, C. Romagnani, A. Rubartelli, J. Ruland, A. Saalmüller, Y. Saeys, T. Saito, S. Sakaguchi, F. Sala-de-Oyanguren, Y. Samstag, S. Sanderson, I. Sandrock, A. Santoni, R.B. Sanz, M. Saresella, C. Sautes-Fridman, B. Sawitzki, L. Schadt, A. Scheffold, H.U. Scherer, M. Schiemann, F.A. Schildberg, E. Schimisky, A. Schlitzer, J. Schlosser, S. Schmid, S. Schmitt, K. Schober, D. Schraivogel, W. Schuh, T. Schüler, R. Schulte, A.R. Schulz, S.R. Schulz, C. Scottá, D. Scott-Algara, D.P. Sester, T.V. Shankey, B. Silva-Santos, A.K. Simon, K.M. Sitnik, S. Sozzani, D.E. Speiser, J. Spidlen, A. Stahlberg, A.M. Stall, N. Stanley, R. Stark, C. Stehle, T. Steinmetz, H. Stockinger, Y. Takahama, K. Takeda, L. Tan, A. Tárnok, G. Tiegs, G. Toldi, J. Tornack, E. Traggiai, M. Trebak, T.I.M. Tree, J. Trotter, J. Trowsdale, M. Tsoumakidou, H. Ulrich, S. Urbanczyk, W. van de Veen, M. van den Broek, E. van der Pol, S. Van Gassen, G. Van Isterdael, R.A.W. van Lier, M. Veldhoen, S. Vento-Asturias, P. Vieira, D. Voehringer, H.-D. Volk, A. von Borstel, K. von Volkmann, A. Waisman, R. V Walker, P.K. Wallace, S.A. Wang, X.M. Wang, M.D. Ward, K.A. Ward-Hartstonge, K. Warnatz, G. Warnes, S. Warth, C. Waskow, J. V Watson, C. Watzl, L. Wegener, T. Weisenburger, A. Wiedemann, J. Wienands, A. Wilharm, R.J. Wilkinson, G. Willimsky, J.B. Wing, R. Winkelmann, T.H. Winkler, O.F. Wirz, A. Wong, P. Wurst, J.H.M. Yang, J. Yang, M. Yazdanbakhsh, L. Yu, A. Yue, H. Zhang, Y. Zhao, S.M. Ziegler, C. Zielinski, J. Zimmermann, A. Zychlinsky, Guidelines for the use of flow cytometry and cell sorting in immunological studies (second edition)., Eur. J. Immunol. 49 (2019) 1457–1973. https://doi.org/10.1002/eji.201970107.

[56] A. Parihar, T.D. Eubank, A.I. Doseff, Monocytes and macrophages regulate immunity through dynamic networks of survival and cell death., J. Innate Immun. 2 (2010) 204–15. https://doi.org/10.1159/000296507.

[57] N. Kim-Campbell, H. Gomez, H. Bayir, Chapter 20 - Cell Death Pathways: Apoptosis and Regulated Necrosis, in: C. Ronco, R. Bellomo, J.A. Kellum, Z.B.T.-C.C.N. (Third E. Ricci (Eds.), Content Repository Only!, Philadelphia, 2019: pp. 113-121.e2. https://doi.org/https://doi.org/10.1016/B978-0-323-44942-7.00020-0.

[58] U. Natarajan, T. Venkatesan, V. Radhakrishnan, S. Samuel, A. Rathinavelu, Differential Mechanisms of Cell Death Induced by HDAC Inhibitor SAHA and MDM2 Inhibitor RG7388 in MCF-7 Cells, Cells. 8 (2018) 8. https://doi.org/10.3390/cells8010008.

[59] L. DiPeso, D.X. Ji, R.E. Vance, J. V Price, Cell death and cell lysis are separable events during pyroptosis, Cell Death Discov. 3 (2017) 17070. https://doi.org/10.1038/cddiscovery.2017.70.

[60] C.J. Kuckleburg, M.J. Sylte, T.J. Inzana, L.B. Corbeil, B.J. Darien, C.J. Czuprynski, Bovine platelets activated by Haemophilus somnus and its LOS induce apoptosis in bovine endothelial cells, Microb. Pathog. 38 (2005) 23–32. https://doi.org/https://doi.org/10.1016/j.micpath.2004.10.006.

[61] D. V. Krysko, T. Vanden Berghe, K. D'Herde, P. Vandenabeele, Apoptosis and necrosis: Detection, discrimination and phagocytosis, Methods. 44 (2008) 205–221. https://doi.org/10.1016/j.ymeth.2007.12.001.

[62] C. Catozzi, G. Ávila, V. Zamarian, D. Pravettoni, G. Sala, F. Ceciliani, N. Lacetera, C. Lecchi, In-vitro effect of heat stress on bovine monocytes lifespan and polarization, Immunobiology. (2019) 151888. https://doi.org/10.1016/j.imbio.2019.11.023.

[63] C.D. Fischer, J.K. Beatty, S.C. Duquette, D.W. Morck, M.J. Lucas, A.G. Buret, Direct and indirect anti-inflammatory effects of tulathromycin in bovine macrophages: inhibition of CXCL-8 secretion, induction of apoptosis, and promotion of efferocytosis, Antimicrob. Agents Chemother. 57 (2013) 1385–1393. https://doi.org/10.1128/AAC.01598-12.

[64] M. Mulongo, T. Prysliak, E. Scruten, S. Napper, J. Perez-Casal, In vitro infection of bovine monocytes with Mycoplasma bovis delays apoptosis and suppresses production of gamma interferon and tumor necrosis factor alpha but not interleukin-10, Infect. Immun. 82 (2014) 62–71. https://doi.org/10.1128/IAI.00961-13.

[65] R. Chen, R. Kang, X.-G. Fan, D. Tang, Release and activity of histone in diseases, Cell Death Dis. 5 (2014) e1370–e1370. https://doi.org/10.1038/cddis.2014.337.

[66] M. Denis, D.N. Wedlock, B.M. Buddle, IFN-γ enhances bovine macrophage responsiveness to Mycobacterium bovis: Impact on bacterial replication, cytokine release and macrophage apoptosis, Immunol. Cell Biol. 83 (2005) 643–650. https://doi.org/10.1111/j.1440-1711.2005.01386.x.

[67] E. Silk, H. Zhao, H. Weng, D. Ma, The role of extracellular histone in organ injury, Cell Death Dis. 8 (2017) e2812–e2812. https://doi.org/10.1038/cddis.2017.52.

[68] F.K.-M. Chan, K. Moriwaki, M.J. De Rosa, Detection of necrosis by release of lactate dehydrogenase activity, Methods Mol. Biol. 979 (2013) 65–70. https://doi.org/10.1007/978-1-62703-290-2_7.

[69] D. Scalia, N. Lacetera, U. Bernabucci, K. Demeyere, L. Duchateau, C. Burvenich, In Vitro Effects of Nonesterified Fatty Acids on Bovine Neutrophils Oxidative Burst and Viability1, J. Dairy Sci. 89 (2006) 147–154. https://doi.org/https://doi.org/10.3168/jds.S0022-0302(06)72078-1.

[70] Z. Sladek, D. Rysanek, Apoptosis of resident and inflammatory macrophages before and during the inflammatory response of the virgin bovine mammary gland, Acta Vet. Scand. 52 (2010) 12. https://doi.org/10.1186/1751-0147-52-12.

[71] J.-I. Abe, C. Morrell, Pyroptosis as a Regulated Form of Necrosis: PI+/Annexin V-/High Caspase 1/Low Caspase 9 Activity in Cells = Pyroptosis?, Circ. Res. 118 (2016) 1457–1460. https://doi.org/10.1161/CIRCRESAHA.116.308699.

[72] N. Li, R. Richoux, M.-H. Perruchot, M. Boutinaud, J.-F. Mayol, V. Gagnaire, Flow Cytometry

Approach to Quantify the Viability of Milk Somatic Cell Counts after Various Physico-Chemical Treatments., PLoS One. 10 (2015) e0146071. https://doi.org/10.1371/journal.pone.0146071.

[73] T. Decker, M.-L. Lohmann-Matthes, A quick and simple method for the quantitation of lactate dehydrogenase release in measurements of cellular cytotoxicity and tumor necrosis factor (TNF) activity, J. Immunol. Methods. 115 (1988) 61–69. https://doi.org/https://doi.org/10.1016/0022-1759(88)90310-9.

[74] A.B. den Hartigh, S.L. Fink, Detection of Inflammasome Activation and Pyroptotic Cell Death in Murine Bone Marrow-derived Macrophages, J. Vis. Exp. (2018) 57463. https://doi.org/10.3791/57463.

[75] M. van Engeland, L.J. Nieland, F.C. Ramaekers, B. Schutte, C.P. Reutelingsperger, Annexin V-affinity assay: a review on an apoptosis detection system based on phosphatidylserine exposure., Cytometry. 31 (1998) 1–9. https://doi.org/10.1002/(sici)1097-0320(19980101)31:1<1::aid-cyto1>3.0.co;2-r.

[76] L.C. Crowley, N.J. Waterhouse, Detecting Cleaved Caspase-3 in Apoptotic Cells by Flow Cytometry, Cold Spring Harb. Protoc. 2016 (2016) pdb.prot087312. https://doi.org/10.1101/pdb.prot087312.

[77] E.A. Miao, J. V Rajan, A. Aderem, Caspase-1-induced pyroptotic cell death., Immunol. Rev. 243 (2011) 206–14. https://doi.org/10.1111/j.1600-065X.2011.01044.x.

[78] D. WU, Signaling mechanisms for regulation of chemotaxis, Cell Res. 15 (2005) 52–56. https://doi.org/10.1038/sj.cr.7290265.

[79] H.-C. Chen, Boyden Chamber Assay BT - Cell Migration: Developmental Methods and Protocols, in: J.-L. Guan (Ed.), Humana Press, Totowa, NJ, 2005: pp. 15–22. https://doi.org/10.1385/1-59259-860-9:015.

[80] W.A. Marasco, S.H. Phan, H. Krutzsch, H.J. Showell, D.E. Feltner, R. Nairn, E.L. Becker, P.A. Ward, Purification and identification of formyl-methionyl-leucyl-phenylalanine as the major peptide neutrophil chemotactic factor produced by Escherichia coli., J. Biol. Chem. 259 (1984) 5430–9. http://www.ncbi.nlm.nih.gov/pubmed/6371005.

[81] H.Y. Lee, M. Lee, Y.-S. Bae, Formyl Peptide Receptors in Cellular Differentiation and Inflammatory Diseases., J. Cell. Biochem. 118 (2017) 1300–1307. https://doi.org/10.1002/jcb.25877.

[82] E.J. Carroll, R. Mueller, L. Panico, Chemotactic factors for bovine leukocytes., Am. J. Vet. Res. 43 (1982) 1661–4. http://www.ncbi.nlm.nih.gov/pubmed/6816108.

[83] G.D. Gray, K.A. Knight, R.D. Nelson, M.J. Herron, Chemotactic requirements of bovine leukocytes., Am. J. Vet. Res. 43 (1982) 757–9. http://www.ncbi.nlm.nih.gov/pubmed/6283962.

[84] C. Lecchi, F. Ceciliani, S. Bernasconi, F. Franciosi, V. Bronzo, P. Sartorelli, Bovine alpha-1 acid glycoprotein can reduce the chemotaxis of bovine monocytes and modulate CD18 expression, Vet. Res. 39 (2008) 50. https://doi.org/10.1051/vetres:2008027.

[85] S. McClelland, C. Cox, R. O'Connor, M. de Gaetano, C. McCarthy, L. Cryan, D. Fitzgerald, O. Belton, Conjugated linoleic acid suppresses the migratory and inflammatory phenotype of the monocyte/macrophage cell, Atherosclerosis. 211 (2010) 96–102. https://doi.org/10.1016/j.atherosclerosis.2010.02.003.

[86] M.R. V Walter, D.W. Morck, Chemotaxis, phagocytosis, and oxidative metabolism in bovine macrophages exposed to a novel interdigital phlegmon (foot rot) lesion isolate, Porphyromonas levii., Am. J. Vet. Res. 63 (2002) 757–62. https://doi.org/10.2460/ajvr.2002.63.757.

[87] N. Gomez-Lopez, F. Vadillo-Ortega, G. Estrada-Gutierrez, Combined Boyden-Flow Cytometry Assay Improves Quantification and Provides Phenotypification of Leukocyte Chemotaxis, PLoS One. 6 (2011) e28771. https://doi.org/10.1371/journal.pone.0028771.

[88] E. Rendra, V. Riabov, D.M. Mossel, T. Sevastyanova, M.C. Harmsen, J. Kzhyshkowska, Reactive oxygen species (ROS) in macrophage activation and function in diabetes., Immunobiology. 224 (2019) 242–253. https://doi.org/10.1016/j.imbio.2018.11.010.

[89] L. Schlesinger, M. Arevalo, S. Arredondo, B. Lönnerdal, A. Stekel, Zinc supplementation impairs monocyte function., Acta Paediatr. 82 (1993) 734–8. https://doi.org/10.1111/j.1651-2227.1993.tb12548.x.

[90] C.F. Batista, M.G. Blagitz, H.G. Bertagnon, R.C. Gomes, K.R. Santos, A.M.M.P. Della Libera, Evolution of phagocytic function in monocytes and neutrophils blood cells of healthy calves., J. Dairy Sci. 98 (2015) 8882–8. https://doi.org/10.3168/jds.2015-9573.

[91] D. Schulz, Y. Severin, V.R.T. Zanotelli, B. Bodenmiller, In-Depth Characterization of Monocyte-Derived Macrophages using a Mass Cytometry-Based Phagocytosis Assay., Sci. Rep. 9 (2019) 1925. https://doi.org/10.1038/s41598-018-38127-9.

[92] C. Menge, B. Neufeld, W. Hirt, N. Schmeer, R. Bauerfeind, G. Baljer, L.H. Wieler, Compensation of preliminary blood phagocyte immaturity in the newborn calf., Vet. Immunol. Immunopathol. 62 (1998) 309–21. https://doi.org/10.1016/s0165-2427(98)00109-3.

[93] A.L. Rivas, R. Tadevosyan, R.C. Gorewit, K.L. Anderson, R. Lyman, R.N. González, Relationships between the phagocytic ability of milk macrophages and polymorphonuclear cells and somatic cell counts in uninfected cows., Can. J. Vet. Res. 70 (2006) 68–74. http://www.ncbi.nlm.nih.gov/pubmed/16548336.

[94] D.I. Bounous, F.M. Enright, K.A. Gossett, C.M. Berry, Phagocytosis, killing, and oxidant production

by bovine monocyte-derived macrophages upon exposure to Brucella abortus strain 2308., Vet. Immunol. Immunopathol. 37 (1993) 243–56. https://doi.org/10.1016/0165-2427(93)90197-c.

[95] D.A. Drevets, B.P. Canono, P.A. Campbell, Measurement of bacterial ingestion and killing by macrophages., Curr. Protoc. Immunol. 109 (2015) 14.6.1-14.6.17. https://doi.org/10.1002/0471142735.im1406s109.

[96] C.F. Bassøe, I. Smith, S. Sørnes, A. Halstensen, A.K. Lehmann, Concurrent measurement of antigen- and antibody-dependent oxidative burst and phagocytosis in monocytes and neutrophils., Methods. 21 (2000) 203–20. https://doi.org/10.1006/meth.2000.1001.

[97] A.H. Kampen, T. Tollersrud, S. Larsen, J.A. Roth, D.E. Frank, A. Lund, Repeatability of flow cytometric and classical measurement of phagocytosis and respiratory burst in bovine polymorphonuclear leukocytes., Vet. Immunol. Immunopathol. 97 (2004) 105–14. https://doi.org/10.1016/j.vetimm.2003.08.018.

[98] J. Hussen, A. Düvel, O. Sandra, D. Smith, I.M. Sheldon, P. Zieger, H.-J. Schuberth, Phenotypic and Functional Heterogeneity of Bovine Blood Monocytes, PLoS One. 8 (2013) e71502. https://doi.org/10.1371/journal.pone.0071502.

[99] M. Rinaldi, P. Moroni, M.J. Paape, D.D. Bannerman, Evaluation of assays for the measurement of bovine neutrophil reactive oxygen species., Vet. Immunol. Immunopathol. 115 (2007) 107–25. https://doi.org/10.1016/j.vetimm.2006.09.009.

[100] L.F. Pisani, C. Lecchi, G. Invernizzi, P. Sartorelli, G. Savoini, F. Ceciliani, In vitro modulatory effect of omega-3 polyunsaturated fatty acid (EPA and DHA) on phagocytosis and ROS production of goat neutrophils., Vet. Immunol. Immunopathol. 131 (2009) 79–85. https://doi.org/10.1016/j.vetimm.2009.03.018.

[101] T. Münzel, I.B. Afanas'ev, A.L. Kleschyov, D.G. Harrison, Detection of Superoxide in Vascular Tissue, Arterioscler. Thromb. Vasc. Biol. 22 (2002) 1761–1768. https://doi.org/10.1161/01.ATV.0000034022.11764.EC.

[102] C. Lecchi, G. Invernizzi, A. Agazzi, M. Ferroni, L.F. Pisani, G. Savoini, F. Ceciliani, In vitro modulation of caprine monocyte immune functions by ω-3 polyunsaturated fatty acids., Vet. J. 189 (2011) 353–5. https://doi.org/10.1016/j.tvjl.2010.09.001.

[103] H.B. Ohmann, L.A. Babiuk, In vitro generation of hydrogen peroxide and of superoxide anion by bovine polymorphonuclear neutrophilic granulocytes, blood monocytes, and alveolar macrophages, Inflammation. 8 (1984) 251–275. https://doi.org/10.1007/BF00916415.

[104] P.C. Calder, S. Kew, The immune system: a target for functional foods?, Br. J. Nutr. 88 (2002) S165. https://doi.org/10.1079/BJN2002682.

[105] C.S. Kurokawa, J.P. Araujo Jr., A.M.V.C. Soares, M.F. Sugizaki, M.T.S. Peraçoli, Pro- and Anti-Inflammatory Cytokines Produced by Human Monocytes Challenged In Vitro with Paracoccidioides brasiliensis, Microbiol. Immunol. 51 (2007) 421–428. https://doi.org/10.1111/j.1348-0421.2007.tb03929.x.

[106] R. van Furth, Human monocytes and cytokines, Res. Immunol. 149 (1998) 719–720. https://doi.org/https://doi.org/10.1016/S0923-2494(99)80045-5.

[107] L. Chávez-galán, M.L. Olleros, D. Vesin, I. Garcia, R.A. Harris, Much more than M1 and M2 macrophages , there are also CD169 + and TCR + macrophages, 6 (2015) 1–15. https://doi.org/10.3389/fimmu.2015.00263.

[108] Y. Zhuang, W. Mwangi, W.C. Brown, W.C. Davis, J.C. Hope, G.H. Palmer, Characterization of a phenotypically unique population of CD13+ dendritic cells resident in the spleen., Clin. Vaccine Immunol. 13 (2006) 1064–9. https://doi.org/10.1128/CVI.00178-06.

[109] M. V Palmer, T.C. Thacker, M.M. Rabideau, G.J. Jones, C. Kanipe, H.M. Vordermeier, W. Ray Waters, Biomarkers of cell-mediated immunity to bovine tuberculosis, Vet. Immunol. Immunopathol. 220 (2020) 109988. https://doi.org/https://doi.org/10.1016/j.vetimm.2019.109988.

[110] N. Bernitz, C. Clarke, E.O. Roos, W.J. Goosen, D. Cooper, P.D. van Helden, S.D.C. Parsons, M.A. Miller, Detection of Mycobacterium bovis infection in African buffaloes (Syncerus caffer) using QuantiFERON®-TB Gold (QFT) tubes and the Qiagen cattletype® IFN-gamma ELISA, Vet. Immunol. Immunopathol. 196 (2018) 48–52. https://doi.org/https://doi.org/10.1016/j.vetimm.2017.12.010.

[111] A. Gupta, K. Gupta, G.D. Leishangthem, M.S. Bal, N.K. Sood, A. Singh, Molecular and pathological studies on natural cases of bovine theileriosis, J. Parasit. Dis. 41 (2017) 211–218. https://doi.org/10.1007/s12639-016-0781-6.

[112] C. Harte, A.L. Gorman, S. McCluskey, M. Carty, A.G. Bowie, C.J. Scott, K.G. Meade, E.C. Lavelle, Alum Activates the Bovine NLRP3 Inflammasome, Front. Immunol. . 8 (2017) 1494.

[113] L. De Pablo-Maiso, I. Echeverría, S. Rius-Rocabert, L. Luján, D. Garcin, D. De Andrés, E. Nistal-Villán, R. Reina, Sendai virus, a strong inducer of anti-lentiviral state in ovine cells, Vaccines. 8 (2020) 1–16. https://doi.org/10.3390/vaccines8020206.

[114] S. Rius-Rocabert, J.L. Presa, S. Esteban-Rubio, A. Ayuso-Sacido, E. Nistal-Villan, A Digital Method to Quantify Type I Interferon, J. Interf. Cytokine Res. 39 (2019) 711–719. https://doi.org/10.1089/jir.2019.0046.

[115] A. Isaacs, J. Lindenmann, C.H. Andrewes, Virus interference. I. The interferon, Proc. R. Soc. London. Ser. B - Biol. Sci. 147 (1957) 258–267. https://doi.org/10.1098/rspb.1957.0048.

[116] E. Voigt, B. Inankur, A. Baltes, J. Yin, A quantitative infection assay for human type I, II, and III interferon antiviral activities, Virol. J. 10 (2013) 224. https://doi.org/10.1186/1743-422X-10-224.

[117] D.A. Magee, K.M. Conlon, N.C. Nalpas, J.A. Browne, C. Pirson, C. Healy, K.E. McLoughlin, J. Chen, H.M. Vordermeier, E. Gormley, D.E. MacHugh, S. V. Gordon, Innate cytokine profiling of bovine alveolar macrophages reveals commonalities and divergence in the response to Mycobacterium bovis and Mycobacterium tuberculosis infection, Tuberculosis. 94 (2014) 441–450. https://doi.org/10.1016/j.tube.2014.04.004.

[118] J. Hellemans, J. Vandesompele, Selection of Reliable Reference Genes for RT-qPCR Analysis, in: 2014: pp. 19–26. https://doi.org/10.1007/978-1-4939-0733-5_3.

[119] C. Puech, L. Dedieu, I. Chantal, V. Rodrigues, Design and evaluation of a unique SYBR Green real-time RT-PCR assay for quantification of five major cytokines in cattle, sheep and goats, BMC Vet. Res. 11 (2015) 65. https://doi.org/10.1186/s12917-015-0382-0.

[120] S.A. Bustin, V. Benes, J.A. Garson, J. Hellemans, J. Huggett, M. Kubista, R. Mueller, T. Nolan, M.W. Pfaffl, G.L. Shipley, J. Vandesompele, C.T. Wittwer, The MIQE guidelines: minimum information for publication of quantitative real-time PCR experiments., Clin. Chem. 55 (2009) 611–22. https://doi.org/10.1373/clinchem.2008.112797.

[121] A.S. Stephens, S.R. Stephens, N.A. Morrison, Internal control genes for quantitative RT-PCR expression analysis in mouse osteoblasts, osteoclasts and macrophages, BMC Res. Notes. 4 (2011). https://doi.org/10.1186/1756-0500-4-410.

[122] M.B. Maeß, S. Sendelbach, S. Lorkowski, Selection of reliable reference genes during THP-1 monocyte differentiation into macrophages, BMC Mol. Biol. 11 (2010) 1–8. https://doi.org/10.1186/1471-2199-11-90.

[123] C. Lecchi, F. Dilda, P. Sartorelli, F. Ceciliani, Widespread expression of SAA and Hp RNA in bovine tissues after evaluation of suitable reference genes, Vet. Immunol. Immunopathol. 145 (2012) 556–562. https://doi.org/10.1016/j.vetimm.2011.12.017.

[124] M.W. Pfaffl, A. Tichopad, C. Prgomet, T.P. Neuvians, Determination of stable housekeeping genes, differentially regulated target genes and sample integrity: BestKeeper--Excel-based tool using pair-wise correlations, Biotechnol. Lett. 26 (2004) 509–515. https://doi.org/10.1023/b:bile.0000019559.84305.47.

[125] D. Garcia-Crespo, R.A. Juste, A. Hurtado, Selection of ovine housekeeping genes for normalisation by real-time RT-PCR; analysis of PrP gene expression and genetic susceptibility to scrapie, BMC Vet. Res. 1 (2005) 3. https://doi.org/10.1186/1746-6148-1-3.

[126] J. Jarczak, J. Kaba, E. Bagnicka, The validation of housekeeping genes as a reference in quantitative

Real Time PCR analysis: Application in the milk somatic cells and frozen whole blood of goats infected with caprine arthritis encephalitis virus, Gene. 549 (2014) 280–285. https://doi.org/https://doi.org/10.1016/j.gene.2014.07.063.

[127] J. Yperman, G. De Visscher, P. Holvoet, W. Flameng, Beta-actin cannot be used as a control for gene expression in ovine interstitial cells derived from heart valves, J. Heart Valve Dis. 13 (2004) 848–853.

[128] M.M. Elnaggar, G.S. Abdellrazeq, M. Sester, S.A. Khaliel, M. Singh, H.A. Torky, W.C. Davis, Development of an improved ESAT-6 and CFP-10 peptide-based cytokine flow cytometric assay for bovine tuberculosis, Comp. Immunol. Microbiol. Infect. Dis. 42 (2015) 1–7. https://doi.org/10.1016/j.cimid.2015.07.005.

[129] P. Lovelace, H.T. Maecker, Multiparameter intracellular cytokine staining., Methods Mol. Biol. 699 (2011) 165–78. https://doi.org/10.1007/978-1-61737-950-5_8.

[130] Y. Corripio-Miyar, J. Hope, C.J. McInnes, S.R. Wattegedera, K. Jensen, Y. Pang, G. Entrican, E.J. Glass, Phenotypic and functional analysis of monocyte populations in cattle peripheral blood identifies a subset with high endocytic and allogeneic T-cell stimulatory capacity, Vet. Res. 46 (2015) 112. https://doi.org/10.1186/s13567-015-0246-4.

[131] B. Pomeroy, A. Sipka, J. Hussen, M. Eger, Y. Schukken, H.-J. Schuberth, Counts of bovine monocyte subsets prior to calving are predictive for postpartum occurrence of mastitis and metritis, Vet. Res. 48 (2017) 13. https://doi.org/10.1186/s13567-017-0415-8.

[132] A.N. Barclay, M.H. Brown, The SIRP family of receptors and immune regulation., Nat. Rev. Immunol. 6 (2006) 457–64. https://doi.org/10.1038/nri1859.

[133] A.M. Nagi, L.A. Babiuk, Characterization of surface markers of bovine gut mucosal leukocytes using monoclonal antibodies., Vet. Immunol. Immunopathol. 22 (1989) 1–14. https://doi.org/10.1016/0165-2427(89)90159-1.

[134] A. Saalmüller, J.K. Lunney, C. Daubenberger, W. Davis, U. Fischer, T.W. Göbel, P. Griebel, E. Hollemweguer, T. Lasco, R. Meister, H.-J. Schuberth, K. Sestak, P. Sopp, F. Steinbach, W. Xiao-Wei, B. Aasted, Summary of the animal homologue section of HLDA8., Cell. Immunol. 236 (n.d.) 51–8. https://doi.org/10.1016/j.cellimm.2005.08.009.

[135] B. Brando, D. Barnett, G. Janossy, F. Mandy, B. Autran, G. Rothe, B. Scarpati, G. D'Avanzo, J.L. D'Hautcourt, R. Lenkei, G. Schmitz, A. Kunkl, R. Chianese, S. Papa, J.W. Gratama, Cytofluorometric methods for assessing absolute numbers of cell subsets in blood. European Working Group on Clinical Cell Analysis., Cytometry. 42 (2000) 327–46. https://doi.org/10.1002/1097-0320(20001215)42:6<327::aid-cyto1000>3.0.co;2-f.

[136] F. Grandoni, M.M. Elnaggar, G.S. Abdellrazeq, F. Signorelli, L.M. Fry, C. Marchitelli, V. Hulubei, S.A. Khaliel, H.A. Torky, W.C. Davis, Characterization of leukocyte subsets in buffalo (Bubalus bubalis) with cross-reactive monoclonal antibodies specific for bovine MHC class I and class II molecules and leukocyte differentiation molecules, Dev. Comp. Immunol. 74 (2017) 101–109. https://doi.org/10.1016/j.dci.2017.04.013.

[137] M.M. Elnaggar, G.S. Abdellrazeq, S.K. Venn-Watson, E.D. Jensen, V. Hulubei, L.M. Fry, R.E. Sacco, W.C. Davis, Identification of monoclonal antibodies cross-reactive with bottlenose dolphin orthologues of the major histocompatibility complex and leukocyte differentiation molecules, Vet. Immunol. Immunopathol. 192 (2017) 54–59. https://doi.org/10.1016/j.vetimm.2017.09.007.

[138] S. Thornton, R. Tan, A. Sproles, T. Do, J. Schick, A.A. Grom, M. DeLay, G.S. Schulert, A Multiparameter Flow Cytometry Analysis Panel to Assess CD163 mRNA and Protein in Monocyte and Macrophage Populations in Hyperinflammatory Diseases, J. Immunol. 202 (2019) 1635–1643. https://doi.org/10.4049/jimmunol.1800765.

[139] A. Saalmüller, B. Aasted, Summary of the animal homologue section of HLDA8., Vet. Immunol. Immunopathol. 119 (2007) 2–13. https://doi.org/10.1016/j.vetimm.2007.06.009.

[140] P. Berthon, J. Hopkins, Ruminant cluster CD14., Vet. Immunol. Immunopathol. 52 (1996) 245–8. https://doi.org/10.1016/0165-2427(96)05568-7.

[141] P. Sopp, D. Werling, C. Baldwin, Cross-reactivity of mAbs to human CD antigens with cells from cattle., Vet. Immunol. Immunopathol. 119 (2007) 106–14. https://doi.org/10.1016/j.vetimm.2007.06.014.

[142] N. Goldfinch, P. Reinink, T. Connelley, A. Koets, I. Morrison, I. Van Rhijn, Conservation of mucosal associated invariant T (MAIT) cells and the MR1 restriction element in ruminants, and abundance of MAIT cells in spleen, Vet. Res. 41 (2010) 62. https://doi.org/10.1051/vetres/2010034.

[143] P. Sopp, L.S. Kwong, C.J. Howard, Identification of bovine CD14., Vet. Immunol. Immunopathol. 52 (1996) 323–8. https://doi.org/10.1016/0165-2427(96)05583-3.

[144] V.K. Gupta, I. McConnell, R.G. Dalziel, J. Hopkins, Identification of the sheep homologue of the monocyte cell surface molecule — CD14, Vet. Immunol. Immunopathol. 51 (1996) 89–99. https://doi.org/10.1016/0165-2427(95)05512-6.

[145] P. Boysen, G. Gunnes, D. Pende, M. Valheim, A.K. Storset, Natural killer cells in lymph nodes of healthy calves express CD16 and show both cytotoxic and cytokine-producing properties, Dev. Comp. Immunol. 32 (2008) 773–783. https://doi.org/10.1016/j.dci.2007.11.006.

[146] M.M. Elnaggar, G.S. Abdellrazeq, V. Mack, L.M. Fry, W.C. Davis, K.T. Park, Characterization and use of new monoclonal antibodies to CD11c, CD14, and CD163 to analyze the phenotypic

complexity of ruminant monocyte subsets, Vet. Immunol. Immunopathol. 178 (2016) 57–63. https://doi.org/10.1016/j.vetimm.2016.06.010.

[147] C.J. Howard, G.P. Brooke, D. Werling, P. Sopp, J.C. Hope, K.R. Parsons, R.A. Collins, Dendritic cells in cattle: phenotype and function., Vet. Immunol. Immunopathol. 72 (1999) 119–24. https://doi.org/10.1016/s0165-2427(99)00124-5.

[148] A.M. Nagi, L.A. Babiuk, Peanut agglutinin (PNA): binding and stimulation of bovine intestinal and peripheral blood leukocytes., Vet. Immunol. Immunopathol. 22 (1989) 67–78. https://doi.org/10.1016/0165-2427(89)90164-5.

[149] E.M. Ibeagha-Awemu, A.E. Ibeagha, X. Zhao, The influence of different anticoagulants and sample preparation methods on measurement of mCD14 on bovine monocytes and polymorphonuclear neutrophil leukocytes, BMC Res. Notes. 5 (2012) 93. https://doi.org/10.1186/1756-0500-5-93.

[150] F. Mandy, B. Brando, Enumeration of Absolute Cell Counts Using Immunophenotypic Techniques, Curr. Protoc. Cytom. 13 (2000). https://doi.org/10.1002/0471142956.cy0608s13.

[151] L.C. Davies, P.R. Taylor, Tissue-resident macrophages: then and now., Immunology. 144 (2015) 541–8. https://doi.org/10.1111/imm.12451.

[152] M. Hesketh, K.B. Sahin, Z.E. West, R.Z. Murray, Macrophage Phenotypes Regulate Scar Formation and Chronic Wound Healing, Int. J. Mol. Sci. 18 (2017) 1545. https://doi.org/10.3390/ijms18071545.

[153] P. Chandrasekaran, S. Izadjoo, J. Stimely, S. Palaniyandi, X. Zhu, W. Tafuri, D.M. Mosser, Regulatory Macrophages Inhibit Alternative Macrophage Activation and Attenuate Pathology Associated with Fibrosis., J. Immunol. 203 (2019) 2130–2140. https://doi.org/10.4049/jimmunol.1900270.

[154] J. Dunn, ed., Manual of Diagnostic Cytology of the Dog and Cat, Wiley, 2014. https://doi.org/10.1002/9781118823040.

[155] E. Piaton, M. Fabre, I. Goubin-Versini, M.-F. Bretz-Grenier, M. Courtade-Saïdi, S. Vincent, G. Belleannée, F. Thivolet, J. Boutonnat, H. Debaque, J. Fleury-Feith, P. Vielh, C. Egelé, J.-P. Bellocq, J.-F. Michiels, B. Cochand-Priollet, Guidelines for May-Grünwald-Giemsa staining in haematology and non-gynaecological cytopathology: recommendations of the French Society of Clinical Cytology (SFCC) and of the French Association for Quality Assurance in Anatomic and Cytologic Pathology (AFA, Cytopathology. 27 (2016) 359–68. https://doi.org/10.1111/cyt.12323.

[156] M.V. Palmer, T.C. Thacker, W.R. Waters, Analysis of Cytokine Gene Expression using a Novel Chromogenic In-situ Hybridization Method in Pulmonary Granulomas of Cattle Infected Experimentally by Aerosolized Mycobacterium bovis, J. Comp. Pathol. 153 (2015) 150–159. https://doi.org/10.1016/j.jcpa.2015.06.004.

[157] H.-E. Park, H.-T. Park, Y.H. Jung, H.S. Yoo, Gene expression profiles of immune-regulatory genes in whole blood of cattle with a subclinical infection of Mycobacterium avium subsp. paratuberculosis, PLoS One. 13 (2018) e0196502. https://doi.org/10.1371/journal.pone.0196502.

[158] M. V. Palmer, T.C. Thacker, W.R. Waters, Multinucleated giant cell cytokine expression in pulmonary granulomas of cattle experimentally infected with Mycobacterium bovis, Vet. Immunol. Immunopathol. 180 (2016) 34–39. https://doi.org/10.1016/j.vetimm.2016.08.015.

[159] M. V. Palmer, J. Wiarda, C. Kanipe, T.C. Thacker, Early Pulmonary Lesions in Cattle Infected via Aerosolized Mycobacterium bovis, Vet. Pathol. 56 (2019) 544–554. https://doi.org/10.1177/0300985819833454.

[160] G. Ampem, H. Azegrouz, Á. Bacsadi, L. Balogh, S. Schmidt, J. Thuróczy, T. Röszer, Adipose tissue macrophages in non-rodent mammals: a comparative study., Cell Tissue Res. 363 (2016) 461–78. https://doi.org/10.1007/s00441-015-2253-1.

[161] A.L. Rivas, F.W. Quimby, J. Blue, O. Coksaygan, Longitudinal evaluation of bovine mammary gland health status by somatic cell counting, flow cytometry, and cytology., J. Vet. Diagn. Invest. 13 (2001) 399–407. https://doi.org/10.1177/104063870101300506.

[162] P. Ganjei-Azar, M. Nadji, eds., Color Atlas of Immunocytochemistry in Diagnostic Cytology, Springer US, Boston, MA, 2006. https://doi.org/10.1007/978-0-387-32122-6.

[163] H.M. Golbar, T. Izawa, V. Juniantito, C. Ichikawa, M. Tanaka, M. Kuwamura, J. Yamate, Immunohistochemical characterization of macrophages and myofibroblasts in fibrotic liver lesions due to Fasciola infection in cattle., J. Vet. Med. Sci. 75 (2013) 857–65. https://doi.org/10.1292/jvms.12-0536.

[164] M. V Palmer, J. Wiarda, C. Kanipe, T.C. Thacker, Early Pulmonary Lesions in Cattle Infected via Aerosolized Mycobacterium bovis., Vet. Pathol. 56 (2019) 544–554. https://doi.org/10.1177/0300985819833454.

[165] M. Fernández, J. Benavides, P. Castaño, N. Elguezabal, M. Fuertes, M. Muñoz, M. Royo, M.C. Ferreras, V. Pérez, Macrophage Subsets Within Granulomatous Intestinal Lesions in Bovine Paratuberculosis., Vet. Pathol. 54 (2017) 82–93. https://doi.org/10.1177/0300985816653794.

[166] M. Fernández, M. Fuertes, N. Elguezabal, P. Castaño, M. Royo, M.C. Ferreras, J. Benavides, V. Pérez, Immunohistochemical expression of interferon-γ in different types of granulomatous lesions associated with bovine paratuberculosis., Comp. Immunol. Microbiol. Infect. Dis. 51 (2017) 1–8. https://doi.org/10.1016/j.cimid.2017.01.002.

[167] A.W. Newman, A. Miller, F.A. Leal Yepes, E. Bitsko, D. Nydam, S. Mann, The effect of the transition period and postpartum body weight loss on macrophage infiltrates in bovine subcutaneous

adipose tissue, J. Dairy Sci. 102 (2019) 1693–1701. https://doi.org/10.3168/jds.2018-15362.

[168] T. Yamada, M. Kamiya, M. Higuchi, N. Nakanishi, Fat depot-specific differences of macrophage infiltration and cellular senescence in obese bovine adipose tissues., J. Vet. Med. Sci. 80 (2018) 1495–1503. https://doi.org/10.1292/jvms.18-0324.

[169] L.J. Oliveira, P.J. Hansen, Phenotypic characterization of macrophages in the endometrium of the pregnant cow., Am. J. Reprod. Immunol. 62 (2009) 418–26. https://doi.org/10.1111/j.1600-0897.2009.00761.x.

[170] L.J. Oliveira, P.J. Hansen, Deviations in populations of peripheral blood mononuclear cells and endometrial macrophages in the cow during pregnancy., Reproduction. 136 (2008) 481–90. https://doi.org/10.1530/REP-08-0218.

[171] Y. Shimamoto, J. Nio-Kobayashi, H. Watarai, M. Nagano, N. Saito, E. Takahashi, H. Higuchi, A. Kobayashi, T. Kimura, H. Kitamura, Generation and validation of novel anti-bovine CD163 monoclonal antibodies ABM-1A9 and ABM-2D6., Vet. Immunol. Immunopathol. 198 (2018) 6–13. https://doi.org/10.1016/j.vetimm.2018.02.004.

[172] C.J. Jenvey, J.M. Hostetter, A.L. Shircliff, J.R. Stabel, Relationship between the pathology of bovine intestinal tissue and current diagnostic tests for Johne's disease., Vet. Immunol. Immunopathol. 202 (2018) 93–101. https://doi.org/10.1016/j.vetimm.2018.06.012.

[173] C.J. Jenvey, A.L. Shircliff, J.P. Bannantine, J.R. Stabel, Phenotypes of macrophages present in the intestine are impacted by stage of disease in cattle naturally infected with Mycobacterium avium subsp. paratuberculosis., PLoS One. 14 (2019) e0217649. https://doi.org/10.1371/journal.pone.0217649.

[174] C.J. Jenvey, J.M. Hostetter, A.L. Shircliff, J.P. Bannantine, J.R. Stabel, Quantification of Macrophages and Mycobacterium avium Subsp. paratuberculosis in Bovine Intestinal Tissue During Different Stages of Johne's Disease., Vet. Pathol. 56 (2019) 671–680. https://doi.org/10.1177/0300985819844823.

[175] J. De Koster, C. Strieder-Barboza, J. de Souza, A.L. Lock, G.A. Contreras, Short communication: Effects of body fat mobilization on macrophage infiltration in adipose tissue of early lactation dairy cows., J. Dairy Sci. 101 (2018) 7608–7613. https://doi.org/10.3168/jds.2017-14318.

[176] R.K. Nelli, J. De Koster, J.N. Roberts, J. de Souza, A.L. Lock, W. Raphael, D. Agnew, G.A. Contreras, Impact of uterine macrophage phenotype on placental retention in dairy cows., Theriogenology. 127 (2019) 145–152. https://doi.org/10.1016/j.theriogenology.2019.01.011.

[177] A. Sterner-Kock, W. Haider, F. Sacchini, A. Liljander, J. Meens, J. Poole, M. Guschlbauer, M. Heller, J. Naessens, J. Jores, Morphological characterization and immunohistochemical detection of

the proinflammatory cytokines IL-1β, IL-17A, and TNF-α in lung lesions associated with contagious bovine pleuropneumonia., Trop. Anim. Health Prod. 48 (2016) 569–76. https://doi.org/10.1007/s11250-016-0994-9.

[178] C.-J. Li, L.-Y. Sun, C.-Y. Pang, Synergistic protection of N-acetylcysteine and ascorbic acid 2-phosphate on human mesenchymal stem cells against mitoptosis, necroptosis and apoptosis., Sci. Rep. 5 (2015) 9819. https://doi.org/10.1038/srep09819.

Figure Captions

Fig. 1 Bovine peripheral blood smears.

A. Normal round monocyte with a deeply indented nucleus and light blue homogeneous cytoplasm is present in a background of normal erythrocytes. Note the non-vacuolated cytoplasm, not all peripheral blood monocytes contain cytoplasmic vacuoles. Bar=7,2 μm.

B. Large peripheral blood monocyte with light blue non-vacuolated cytoplasm with an irregularly bean-shaped indented nucleus. Bar= 6 μm.

C. Large peripheral blood monocyte with irregular membrane contour and abundant light blue cytoplasm characterized by multiple, variably sized discrete cytoplasmic vacuoles. Bar= 4,9 μm. May-Grünwald Giemsa stain.

Fig. 2 Phase-contrast photomicrographs of cultured monocytes following MACS purification.

A. Monocytes the first day in culture (10%FBS supplemented RPMI media). Bar= 20 μm;

B. Monocytes maintained for two days demonstrating a slight increase in size and shape and size variability. Bar=20 μm.

C. Two monocytes maintained for four days in culture and characterized by variably increased size and presenting with cytoplasmic processes indicative of activation and initial transformation into macrophages. Bar= 10 μm.

Fig. 3. Flow cytometry evaluation of monocytes, before and after sorting.

PBMC are showed in a representative dot plot FSC *vs* SSC based on size and granularity (complexity) before (A) and after MACS separation (D). Monocytes staining with FITC-anti-CD14 antibody is showed before (B) and after sorting (E). Representative histograms of the relative percentage of lymphocytes and monocytes are showed before (C) and after sorting (F). MACS purification gives an enrichment of $CD14^+$ monocytes population > of 98%.

Fig. 4. Flow cytometry detection, by annexin V-FITC/PI, of apoptosis and necrosis on bovine PBMC incubated for 1 h at 37 °C.

On dot plot FSC *vs* SSC, a gate around lymphocytes and monocytes regions was drawn and apoptosis and necrosis in gated events were determined. Live lymphocytes (A) and monocytes (B) are Annexin V and PI double negative (lower left quadrant). At the early stage of apoptosis, the cells bind annexin V while still excluding PI (lower right quadrant). Double positive events are necrotic cells (upper right quadrant). The PI-positive - annexin V negative cells (upper left quadrant) are considered necroptotic cells [178].

Fig. 5. *In vitro* methods to measure chemotaxis

(A) Schematic illustration of the Boyden chamber assay. Cells seeded in the upper chamber migrate through a porous membrane, towards the lower chamber in the response of a chemoattractant gradient concentration. (B) Schematic illustration of a migration transwell plate. The multiwell plate is packaged with permeable and removable cell culture inserts with a porous membrane that allows the migration of the cells towards the medium/chemoattractant-filled lower well. Images were created with BioRender.com".

Fig. 6 Morphological and Immunohistochemical features of bovine macrophages in cytological and tissue specimens

Fig. 6 A Cytology of synovial fluid in a calf with arthritis. Moderately cellular cytological sample illustrating numerous foamy reactive macrophages with variably abundant cytoplasm with numerous cytoplasmic vacuoles admixed with non-degenerate neutrophils in a background of confluent erythrocytes. Joint tap, May-Grünwald Giemsa stain. Bar= 25 µm

Fig. 6 B Cytology of synovial fluid in a calf with arthritis. Large reactive macrophage with heavily vacuolated cytoplasm containing phagocytized apoptotic nuclear material. The macrophage is surrounded by moderately degenerated erythrocytes (crenation) and non-degenerated neutrophils in a granular background of synovial mucins. Joint tap, May-Grünwald Giemsa stain. Bar=7,5 µm

Fig. 6 C Histology of a bovine mesenteric lymph node in a case of paratuberculosis. Sheets of reactive macrophages characterized by varying size, pink to grey cytoplasm and oval nuclei with granular to reticular chromatin and evidence of 1-2 small, basophilic nucleoli are admixed with mature lymphocytes and rare plasma cells. A single multinucleated macrophage with haphazardly arranged nuclei is evident (arrowhead). Haematoxylin and eosin stain. Bar= 14 µm

Fig. 6 D Histology of a bovine thoracic lymph node in a case of Tuberculosis. At the centre of the image, there is a large multinucleated giant macrophage characterized by several nuclei arranged in a horse-show fashion beneath the cell membrane. The cell is surrounded by occasional epithelioid

cells, foamy reactive macrophages with large cytoplasmic well distinct vacuoles and elevated numbers of lymphocytes (left) and lesser plasma cells. Haematoxylin and eosin stain. Bar= 32 μm

Fig. 6 E Bovine small intestine in a case of paratuberculosis. Lamina propria of intestinal villi is substituted and expanded by massive infiltration of large reactive macrophages displacing peripherally and compressing intestinal glands. Haematoxylin and eosin stain. Bar= 170 μm

Fig. 6 F Bovine tongue in a case of wooden tongue (*Actinobacillus lignieresii infection).* Large granuloma composed of reactive macrophages admixed with lesser numbers of neutrophils, eosinophils and lymphocytes and surrounded by fibroblasts and collagen). Haematoxylin and eosin stain. Bar= 75 μm

Fig. 6 G Bovine small intestine in a case of paratuberculosis. Diffuse granulomatous inflammation expanding and substituting the intestinal lamina propria with separation of the epithelial mucosal lining. Large reactive macrophages predominate and associate with lesser numbers of lymphocytes. In the left lower part of the image, an intestinal gland is compressed with gland epithelium lightly infiltrated by eosinophils (arrowhead). Haematoxylin and eosin stain. Bar= 64 μm

Fig. 6 H Bovine small intestine in a case of paratuberculosis. High numbers of acid-fast positive mycobacteria (*Mycobacterium avium* sbsp. paratuberculosis) in the cytoplasm of macrophages and free in the lamina propria. Ziehl – Neelsen stain. Bar= 22 μm

Fig. 6 I Bovine lung in a case of tuberculosis. The image shows the typical stratigraphy of a tuberculoid granuloma substituting the pulmonary parenchyma. The right and central parts of the image represent the extensive central area of caseous necrosis characterized by amorphous eosinophilic and granular basophilic tissue debris. In the left part of the image, necrosis is rimmed by neutrophils, macrophages, multinucleated giant cells of the Langhans cell type and mature lymphocytes. The external portion of the granuloma is composed of fibroblasts and collagen delimiting the granuloma. Haematoxylin and eosin stain. Bar= 196 μm

Fig. 6 J Bovine tongue in a case of wooden tongue (*Actinobacillus lignieresii infection).* Discrete granuloma with central intensely eosinophilic material corresponding to the accumulation of immunoglobulin/immunocomplexes and termed Splendore-Hoeppli phenomenon. Haematoxylin and eosin stain. Bar= 110 μm

Fig 6 K Immunohistochemical stain of a bovine reactive thoracic lymph node. Numerous Iba-1 positive reactive foamy macrophages in the medullary cords. Anti-Iba-1 immunoperoxidase stain, AEC chromogen, hematoxylin counterstain. Bar= 70 μm

Fig 6 L Immunohistochemical stain of a calf lung with bronchopneumonia. Alveolar lumen containing numerous reactive macrophages and rare neutrophils. Two M1 type macrophages intensely expressing TNF–α. Anti-TNF–α immunoperoxidase stain. AEC chromogen, hematoxylin

counterstain. Bar= 18 μm

Figure 1

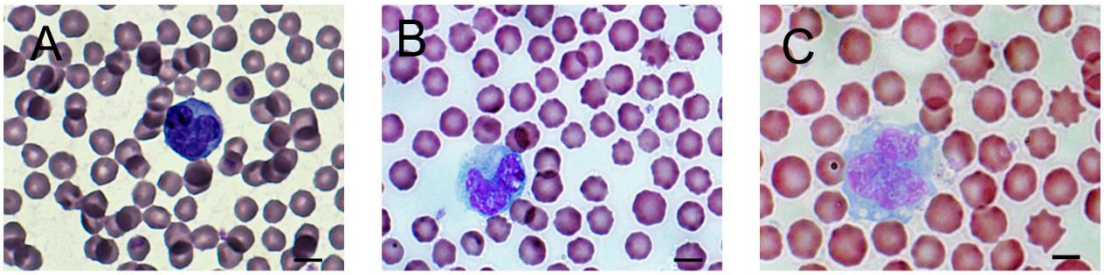

Figure 2

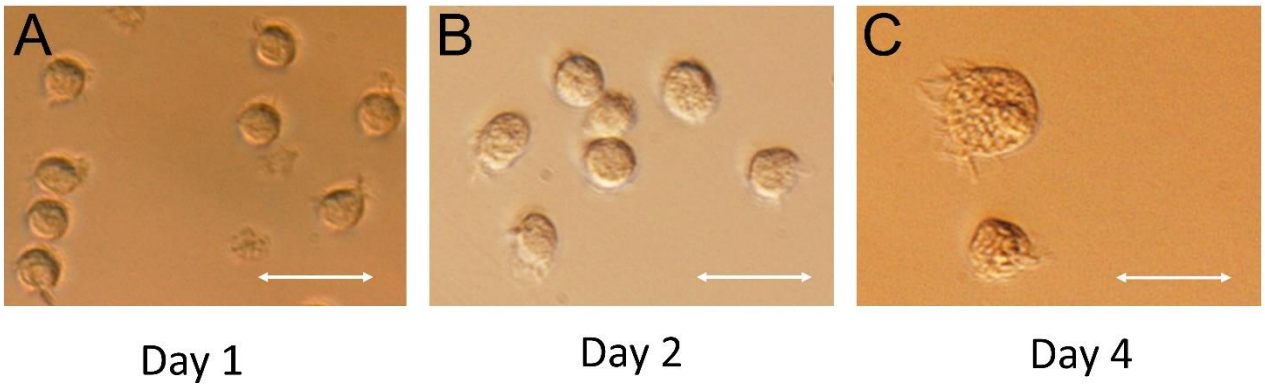

Figure 3

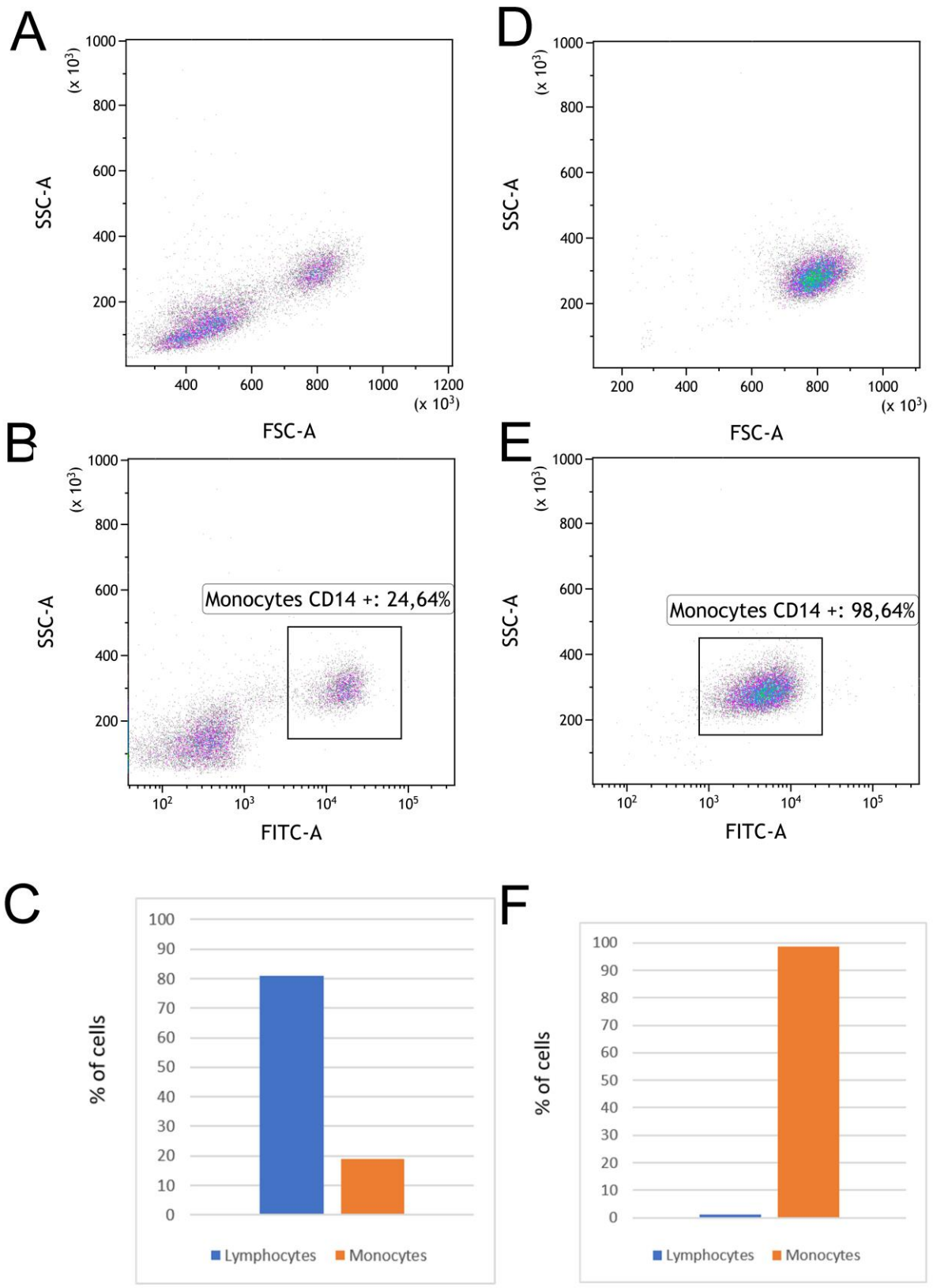
A
D
B
E
C
F
SSC-A
FSC-A
(x 10³)
Monocytes CD14 +: 24,64%
Monocytes CD14 +: 98,64%
FITC-A
% of cells
Lymphocytes
Monocytes

Figure 4

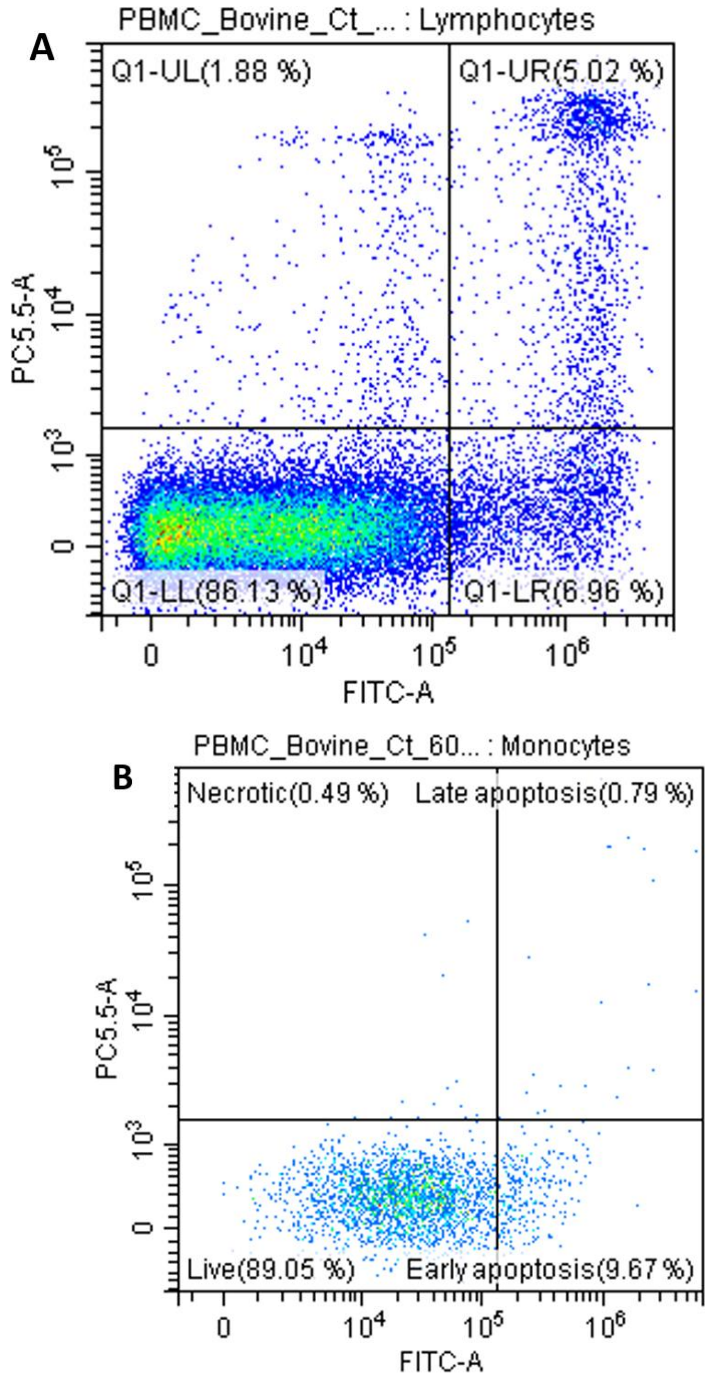
A
PBMC_Bovine_Ct_... : Lymphocytes
Q1-UL(1.88 %)
Q1-UR(5.02 %)
Q1-LL(86.13 %)
Q1-LR(6.96 %)
PC5.5-A
FITC-A
B
PBMC_Bovine_Ct_60... : Monocytes
Necrotic(0.49 %)
Late apoptosis(0.79 %)
Live(89.05 %)
Early apoptosis(9.67 %)
PC5.5-A
FITC-A

Figure 5

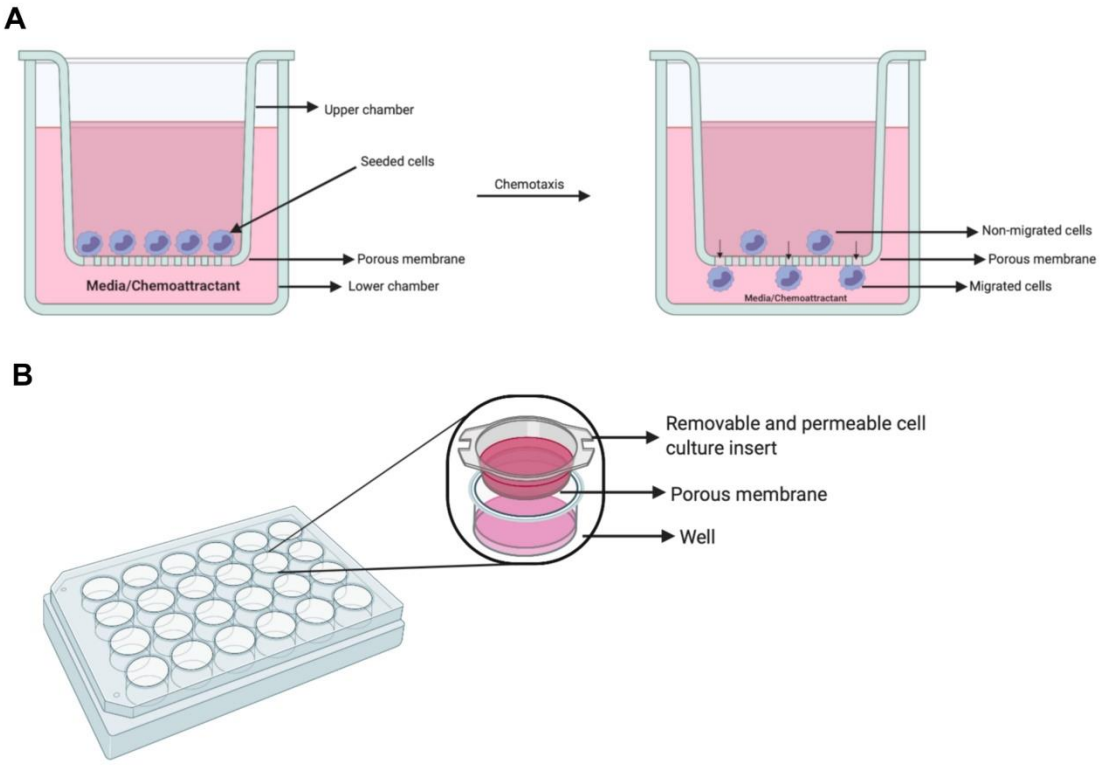
A
Upper chamber
Seeded cells
Porous membrane
Media/Chemoattractant
Lower chamber
Chemotaxis
Non-migrated cells
Porous membrane
Migrated cells
Media/Chemoattractant
B
Removable and permeable cell culture insert
Porous membrane
Well

Figure 6